REPORT NO. 122.

October, 1959.

THE COLLEGE OF AERONAUTICS

CRANFIELD

The dynamic loading of spur gear teeth

- by -

J. H. Dunmore, B.Sc.,
A.C.T.Birm., A.F.Inst.Pet.

SUMMARY

In this report, description of the first stage of some work on the dynamic loading of gear teeth is given. The work has been performed on a power circulating gear rig, using gears of 9 inch P.C.D., 4 D.P., and 1/2 inch face width. The rig is capable of running at pitch line velocities up to 20,000 ft/min. with imposed loads of up to 3,000 lbs/inch of face width. Particular reference is made to the instrumentation problems which were encountered, and to the measurement of the shape of the gears and their associated transmission errors. No attempt is made at a theoretical analysis of the results obtained as this will be the subject of a future report, along with the publication of more results.

CONTENTS

1. Introduction

With the present day demand, in all fields of engineering, for higher speeds and higher working loads, the existence of reliable design criteria becomes important. This is particularly so with problems relating to gears and bearings. This report describes work which is being carried out in the Department of Aircraft Propulsion at the College of Aeronautics, Cranfield, to establish the magnitude of the loads imposed on gear teeth under varying speed and loading conditions.

In the design of gears, two main types of tooth failure have to be considered. These are fracture of the root due to bending fatigue, and failure of the surface, either by scuffing or pitting. Both these types of failure are influenced by tooth loading, and it would appear, therefore, that the accuracy of the estimated life of a gear depends upon the accuracy of the estimated load, for any of the above failures to be avoided. Now, if the load is to be estimated accurately, a reliable estimate must be made of the dynamic loading imposed on the teeth. Various mathematical approaches have been made in an attempt to estimate the loading, but they have been contradictory, and further there has been little experimental evidence to support them. It is the object of this work and its associated research programme to find the effect of several possible variables on the dynamic load. From the results obtained, it is hoped to either substantiate an existing theory or establish a new one. At the very least, there will be some guidance as to which factors are the most important.

2. Description of Test Rig

As has already been stated, the test rig is of the power circulating type. This uses two sets of gears, in effect driven back to back, so that the power requirements are those of the losses encountered in the gears and bearings. A full description of the rig has been given in College of Aeronautics Note No. 75, but for the sake of completeness, will be repeated.

The general arrangement of the rig is shown in Figure 1, and a general view shown in Photograph 1. Four separate bearing housings are mounted in pairs on two small bed-plates which are in turn mounted on one large bed-plate. Each housing contains one double roller bearing and two deep groove ball bearings, which support a short, large diameter, shaft as shown in Figure 2. The bearings used are "ultra-precision bearings" and by suitable alteration of the split spacing ring length, the radial clearance of the roller bearings may be adjusted to any amount by forcing it up its tapered seat. This bearing arrangement gives very accurate radial and axial location of the shaft axis, at the same time giving good accessibility to the test gears. The test gears are housed at (5) (see Fig. 1), and the

slave gears at (4). A full description of the gears is given later.

To insulate the test gears from such extraneous torsional vibrations as do exist, long torsion shafts (3) are used. They are also utilised to impart load to the gear teeth by means of the loading arm (7). This acts on one half of the loading coupling, the other half being rigidly locked for the purposes of loading. A vernier dowel arrangement is used in which one half of the loading coupling has 21 equi-spaced holes on a 6.5 in. diameter and the other half has 20 equi-spaced holes on a similar diameter. This permits the application of the load in increments of 154 lbs/inch of face width.

Two separate lubrication systems are used on the rig, one for the bearings and one for the gears. The bearings are lubricated by oil mist from one lubricator and the gears are supplied with oil from a combined pressure/scavenge pump. The oils used at present are Castrol Hypoy for the gears and Shell Telus 15 for the bearings. The rig is driven by a 50 H.P. Schrage motor, through a 3:1 or 6:1 pulley drive, using a high speed 'Meteor' belt.

2.1. Description of Gears

Test Gears

The basic details of the teeth are as follows :-

P.C.D.	9 inch	No. of teeth	36
Pressure Angle	27°	Face width	1/2 inch
Material	S.82		

Four test gears have been manufactured up to the present. One pair has a pure involute profile; the other has a profile modified to suit current practice at Rolls Royce. As the gears are reversible, both sides of the teeth may be used as pressure faces. One pressure side of each gear has been ground to give the minimum possible pitch errors as given in Table 1. This allows gear faces with nominal tooth spacing to be meshed together in the pure involute and modified involute form. Some of the meshing combinations that can be obtained with these gears are shown in Table II. It is seen that the effects of two basic types of error may be investigated. One is a sudden change in constant adjacent pitch error extending for 9 teeth each side of the investigation point, and the other is an isolated error with 8 teeth each side at nominal pitch. Photograph No. 2 shows the gears with the modified profile in position on the rig.

Slave Gears

The slave gears are helical gears of 8 D.P. and three times the face width of the test gears. This increase in D.P. and face width was chosen

in order that the amount of vibration arising from the slave gears could be kept to a minimum. Photograph No. 3 shows the slave gears mounted in position.

2.2. Description of the Error Measuring Equipment

An ideal pair of gears, operating under ideal conditions, will transfer rotation about the axis of the driving gear into rotation about the axis of the driven gear in a perfectly linear manner. When considering a set of gears operating under varying conditions of load and speed, it is very important to know the deviation from linearity of transfer of angular movement.

In order to measure this deviation, the following device was designed and developed, general views of which are shown in Photographs 7, 8 and 9. Two pulleys, each of 9 inch outside diameter, are mounted, one on each test gear. One of the pulleys consists of a solid circular disc which is mounted rigidly to the gear and the other consists of an annulus of 9 inch outside diameter and a solid circular disc of outside diameter less than the inside diameter of the annulus. The annulus was attached to the disc by means of four radial leaf springs incorporating means for adjustment of the coaxiality of the gear and pulley. A steel flexible belt is arranged, in the manner shown in Photographs 7, 8, and 9 to transfer motion of the first pulley, perfectly linearly to the motion of the second pulley. During the motion of the two test gears, the driving gear of the two test gears will drive the driven gear and consequently any deviation between the motion of the driven pulley and the driving pulley will indicate the magnitude of the lack of linearity in the transfer of angular movement, by the gears. This deviation is shown by movement of the annulus with respect to its solid circular disc. The movement is measured with the aid of a Southern Instruments Magna Gauge, and a galvanometer recorder. The probe of the Magna Gauge, which is in fact an inductive pick-up, is fixed to the annulus and the tip of the probe allowed to rest against a plate fixed to the smaller disc. Early tests fed the output from the Gauge to an ultra-violet galvanometer recorder. The advantage of using the ultra-violet galvanometer recorder was that the paper sensitive to ultra-violet light could be attached to one of the couplings of the rig, and this would serve as the drive for the paper. This avoids any errors arising from changes in velocity whilst turning the rig. This has to be done slowly by hand, as the rig could not be run at very low speeds. It was found that to obtain clear traces suitable for reproduction, a photographic paper, sensitive to white light, had to be used. Another method for measuring these transmission errors is being considered. This consists of using two Southern Instruments Torsiographs fixed to each shaft, and feeding the differential output from each torsiograph to a recording oscilloscope. It is important that the reference position is known accurately, and use is made of the triggering device for the instrumentation. This will be explained in detail in another section.

3. Instrumentation Techniques

At first, two methods for measuring the deflection of the gear teeth relative to the gear shaft were used; firstly movement of the gear teeth relative to the shaft was made to vary the capacity of a small condenser, one plate of which was attached to the tooth and the other fixed rigidly to the shaft (Figure 7 and Photograph No. 4), and secondly a strain gauge was fixed to both sides of a small beam which was made to bend should a tooth move relative to the shaft (see Photograph No. 5). Initially the signal from the condenser was detected by means of a conventional grid-dip oscillator arrangement (Figure 9) but difficulty was experienced with the drift of the oscillator and an alternative method of transmitting this capacity signal was designed. This used another parallel plate condenser, of much greater capacity than the pick-up to transmit the signal to a Southern Instrument F.M. System. A disc is fixed rigidly to the shaft of the instrumented gear and can rotate between two plates with about 0.010 inch clearance between each side of the rotating disc. Figure 8 shows the method used. It is felt that both these methods suffer from lack of high frequency response, due to compliance of the small beam supporting the condenser plate from the test tooth.

The signal from the strain gauges was detected by a normal D.C. Bridge and amplifier feeding into an oscilloscope. Difficulty was experienced using this method, owing to difficulties of sticking the gauges to the beam, and more especially to the problem of mercury slip rings and the associated noise level. The output from the strain gauge was very small, and this resulted in a low signal to noise ratio from the slip ring. With the high amplifications which had to be used to obtain suitable deflections on a recording oscilloscope, this became a problem. It was decided, therefore, to use lead zirconate crystals as strain transducer elements. High outputs can be obtained from these piezo-electric elements and, therefore, the signal to noise ratio will be high. Further, the high frequency response is good. These elements were very successful; they may be attached directly to the side of the gear, if necessary, and have been chosen for further use on the rig.

Another problem arose; that of adequate recording of the phenomena under observation. With the use of a six-channel recording oscilloscope and its recording camera, the important part of the trace, that on which the gear tooth is under load, is very small, even at modest speeds. This is due to limitations of film speed - a maximum of 1200 inches/sec. would be obtained. In view of this, another method of presentation of the phenomena was designed and developed. This system uses a Shackman Camera which takes shots every 0.5 seconds. A triggering signal is taken from the rig, by means of a hole in a disc interrupting a beam of light focussed on to a photo-cell, and fed into an electronic gate. At the same time a 24-volt signal every 0.5 seconds is fed into

the gate and the electronics is arranged so that after the arrival of the first 24-volt pulse, the next signal from the triggering device triggers the oscilloscope and the trace is recorded. The film is then moved on automatically, and nothing happens until the next 24-volts pulse is received, and then the next trigger signal again triggers the oscilloscope beam. This process is repeated throughout the test run. Thus, approximately every $\frac{1}{2}$-second a record is taken as the test tooth meshes. Details of the electronic circuits used are given in Figures 3, 4, 5 and 6. It is seen that a delay is incorporated in order that some compensation for the lead of the triggering signal at different speeds may be given.

The speed of the rig is measured with the aid of a photo-cell and a disc with 60 holes equi-spaced around its circumference. A light source is focussed on to the cell and hence a signal may be obtained from the cell. The signal from the photo-cell is fed to a Dekatron Counter and also to the second beam of the double beam oscilloscope. A signal of known frequency is superimposed on this second beam in order that a time marker may be obtained. A full block diagram of the instrumentation is given in Figure 10.

4. The Measurement of the Individual Gears

This was done by Rolls-Royce, and a chart showing the errors is given in Table 3 and Graphs 1 to 8. As a check, the gears were measured on the Sigma Instrument Company Gear Measuring Device, and the results are shown in Graphs 9 to 12. This machine was described in a paper presented by Professor Loxham (Head of the Department of Economics & Production at the College) to the International Conference on Gearing (Ref. 7). Up to the present, only the pure involute set of gears have been measured on this machine, as the modified profile gears are on the rig, and it was felt desirable to complete the preliminary running on them before disturbing them. Maag profile diagrams for the gears were obtained and are presented following Table 3.

An interesting point arises in that whilst with the built-in errors the measurements from Rolls-Royce and Sigma Instrument Co. agree fairly well, those with the 'perfect' gears show differences. These are being investigated.

5. Method of attaching lead zirconate crystals to the teeth

The lead zirconate crystals were attached to the teeth of the test gear with the aid of Araldite and Hardener. Aluminium powder was mixed into some Araldite and Hardener, in order to make it slightly conducting, and the resulting mixture applied to one side of the crystal which was then fixed and clamped in position on the side of the gear. This was allowed to harden over a period of 24 hours. The appropriate leads can then be soldered to the visible face of the

crystal. Crystals have been attached to the mid point of the strain gauge beam and to the side of the tooth carrying the beam, the crystal being fixed near to the root. The tooth preceding this tooth has a similar crystal attached. Photograph No. 6 shows the position of the crystals.

6. Calibration of the Lead Zirconate Crystals

This may lead to some difficulty, but it is hoped to overcome this by direct comparison with strain gauges. The lead zirconate crystals are an A.C. device, and so tha problem resolves into a comparison with a D.C. device. Strain gauges will be stuck on either side of a fairly stiff beam, and crystals will be stuck by the side of the gauges. The beam will be clamped at one end and calibrated at various amplitudes and frequencies. If the amplitude is known, the stress may be calculated and a direct comparison made between crystals and strain gauges over a range of frequencies. Hence a deflection against output calibration may be made.

7. Results and Discussion

With the gears having the modified profile, corrected to a maximum load of 3,000 lbs/inch face width in position, the following tests have been performed :-

(1) Test using the grid-dip principle for transmitting the capacity signal

(2) Test using the capacity slip ring for transmitting the capacity signal

(3) Test using lead zirconate crystals and the signal from these transmitted by means of a mercury slip ring.

The transmission errors of the gears were measured over a range of loads and the results shown in Appendix 3. The calibration is done in steps of 0.0005 inch.

It is emphasised that this report is preliminary in that it presents only the type of recording that is being obtained from the instrumentation, and that a full theoretical treatment involving a comparison between Professor Tuplin's and Earle Buckingham's method of calculating the dynamic load will be presented at a later date.

Figure 11 shows two capacity transducer records, using the grid-dip method of detecting capacity change, taken with the aid of a drum camera. The traces from left to right on the records are speed marker from the Dowty Tachometer, signal from the capacity transducer, time marker ($\frac{1}{1000}$ second) and strain gauge signal. The single peak in

the capacity signal record represents the meshing of the test tooth.

Figures 12 - 16 inclusive show records, again taken with the aid of a drum type camera, of capacity signal transmitted using the "capacity slip ring". The load has been kept constant at 750 lbs/inch face width, and the speed varied. The traces, reading from left to right, are speed, capacity signal and time marker (0.001 secs.). It will be noted that as the speed is varied, the transducer signal changes in amplitude during the meshing period of the test tooth. For instance, at 1200 r.p.m. the signal is approximately half that at 712 r.p.m. This shows that even with a constant load, there can be marked variations in gear stress with changes in speed. There is also a change in shape of the record with speed. Further, even when the test tooth is not in mesh, it shows a periodic deflection at most of the speeds shown. The reason for this is not yet known.

Considering Figures 18 - 22, these show signals obtained from the lead zirconate crystal, fixed to the side of the tooth having the strain gauge beam attached to it. The signals were obtained by the method described at the bottom of page 4. The loading in this case is the design value of 3,000 lbs/inch face width. Again a marked change in amplitude and shape of the trace is apparent as the speed is changed. The top trace is of pulses representing 6° revolution, the angular pitch of the teeth being 10°. Figures 23 - 29 show the signal recorded in a similar manner, but with the load at 1500 lbs/inch face width. In spite of the load being halved, the transducer signals are little reduced and this would indicate that a large part of the strain at reduced load is due to the dynamic effect of the gears meshing at a load not suited to the profile modifications. Further tests, especially those using involute gears should throw light on the variation of tooth strain with load. A study of Figures 28 and 29, where the records were taken during a run down from maximum speed show that even with small changes in speed, large changes in dynamic load may occur.

Turning now to a study of the error measurements as shown in Appendix 3, it would appear that the profile modification is not quite so good as was at once hoped. Preliminary results, using a system not quite so sensitive as described in this report, had shown better conformity in involute profile at maximum load. It is seen that application of the load has had the effect of reducing the peak of the change period and the change is more gradual but has not brought the gears into involute profile. The bottom trace on the records represents pulses of 6° rotation. It is intended to check the involute gears with the error measuring equipment as soon as possible to check this conclusion.

8. Projected Future Work

(1) Design of a system of loading such that load may be applied whilst the rig is in motion.

(2) Design of a brush type slipring having at least six separate channels.

(3) Development of a system of measuring alternating torque using Moire Fringe Techniques.

9. Immediate Future Work

(1) Check runs with the test gears unmeshed to determine the magnitude of any spurious signal.

(2) Completion of the results from the gears with the profile modification at various speeds and loads.

(3) Results from the involute profile gears at various speeds and loads.

(4) Investigation into the theoretical and practical implications of the results.

(5) Investigation into the torsional vibrations existing in the rig.

(6) Exploration of the shape and size of the strain traces.

10. Acknowledgements

Acknowledgement is made to the following people who have assisted in this work :-

Professor A. G. Smith, Head of the Department of Aircraft Propulsion, for his encouragement and advice.

Professor J. Loxham, Head of the Department of Economics and Production, and the Sigma Instrument Company for measuring the involute profile gears.

Rolls-Royce Ltd., for providing the gears.

Mr. G. W. Jackman and Mr. E. C. Sills of the College of Aeronautics for valuable assistance with the instrumentation.

11. References

1. College of Aeronautics Note No. 75.

2. Merritt, H.E. — Gears. Pitman.

3. Buckingham, E. — Analytical Mechanics of Gears. McGraw Hill.

4. Tuplin, Prof. — Torsional Vibrations. Chapman & Hall.

5. Wilson, Ker. — Practical Solution of Torsional Vibrations Problems, Vol.I. Chapman & Hall.

6. Timoshenko, Prof.S. — Vibration problems in engineering. Van Nostrand.

7. Loxham, J. — Inspection of Cumulative Circular Pitch on High Precision Gears. International Conference on Gearing. Inst. Mech. Engs.

APPENDIX 1

Maximum Sliding Velocity of Test Gears

$$\text{Sliding Velocity } V_s = V \left\{ \frac{1}{R_1} + \frac{1}{R_2} \right\} \left(\sqrt{r_1^2 - R_{b1}^2} - R \sin \phi \right)$$

R_1 and R_2 are radius of pitch circle of gears

V = pitch circle velocity

r_1 = any radius on the gear

R_{b1} = radius of base circle

ϕ = pressure angle

$$\text{Now } R_{b1}^2 = R_{b2}^2 = R_1^2 \cos^2 \phi$$

$$= 4.5^2 \cos^2 27^\circ$$

$$= 16.076$$

for max V_s $r_1 = 4.75$

$$\text{and so } V_s = 20{,}000 \times \frac{2}{4.5} \left\{ \sqrt{4.75^2 - 16.076} - 4.5 \cos 27^\circ \right\}$$

$$= \underline{74.6 \text{ ft/sec.}}$$

Determination of the length of path of contact

$$\text{Length of path of contact} = 2 \left\{ \sqrt{\left\{ \frac{d}{2} + a \right\}^2 - \left\{ \frac{d}{2} \cos \phi \right\}^2} - \frac{d}{2} \sin \phi \right.$$

$$= 2 \left\{ \left(\frac{d_t}{2} \right)^2 - \left(\frac{d_o}{2} \right)^2 \right\}^{\frac{1}{2}} - \frac{d}{2} \sin \phi \left. \right\}$$

where d_t = top diameter

d_o = base circle diameter

$$\text{Length of path of contact} = 2 \left\{ \left\{ 4.7505^2 - 4.0095^2 \right\}^{\frac{1}{2}} - 4.5 \sin 27^\circ \right\}$$

$$= \underline{1.009"}$$

Determination of the change points

Base circle diameter = 8.01906

Base pitch = $\frac{8.01906}{36} \times \pi = 0.6998$

Assuming correct profile modification then the change points will be approximately 0.2" from the pitch point.

Pitch point

0.3	0.2	0.2	0.3
Double Contact	Single Contact		Double Contact

Contact Ratio

Contact Ratio = $\frac{\text{length of path of contact}}{\text{base pitch}}$

$= \frac{1.009}{0.6998} = 1.441$

APPENDIX 2

Torsional Vibration and Resonant Frequency of the Gear Rig

The diagram of the shafting of the rig, with the inertias involved and the equivalent lengths, is as below:-

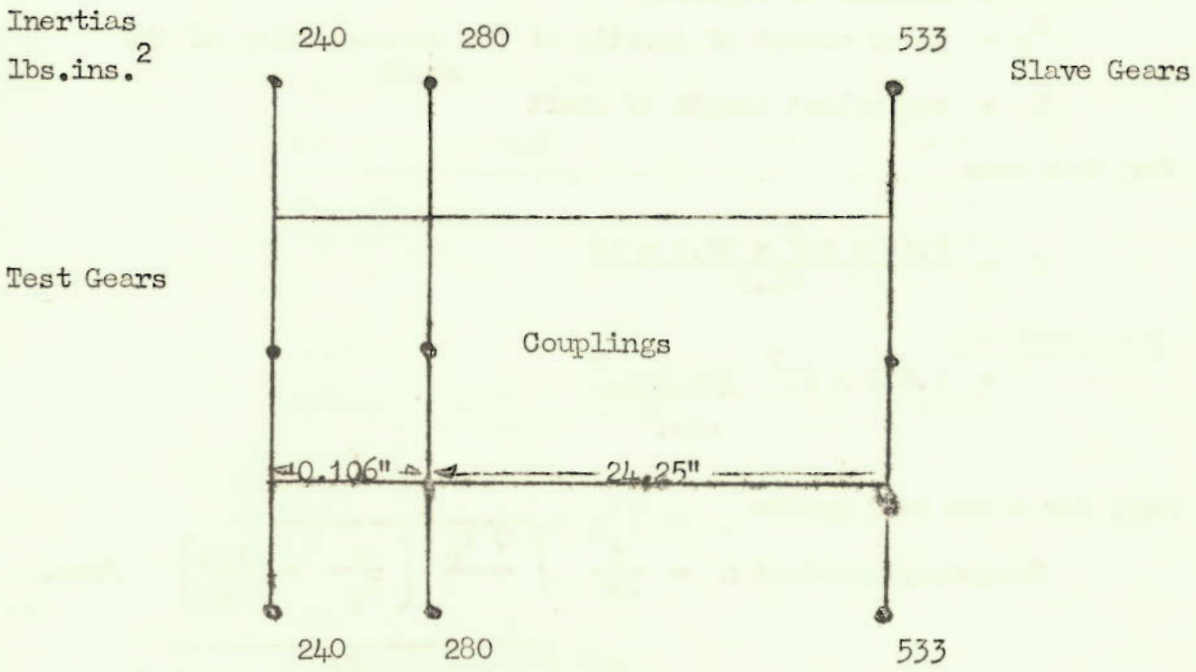

If each line of shafting is considered to be a three mass system, i.e. masses due to the test gears, loading coupling and slave gear, then one line of shafting may be considered. As a first approximation, consider a two mass system as shown below. This is allowable because the equivalent length between the coupling and the test gear is small compared with the equivalent length between the coupling and the slave gear. For this case the inertias of

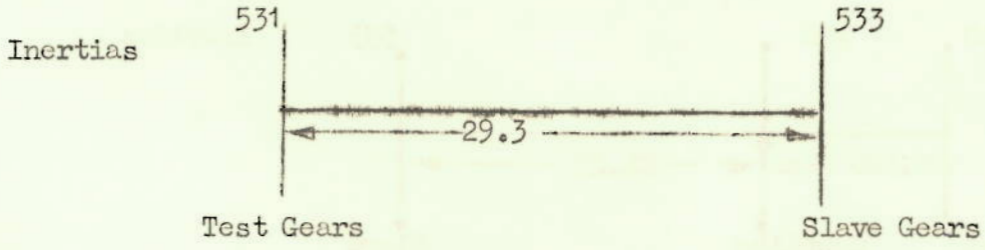

the bearing shafts have been added for this two mass case. Following

Tuplin (Ref. 1) gives

$$\text{Spring Constant } C = \frac{G\ I_p}{L}$$

C = torsional rigidity of shaft
G = modulus of rigidity
L_p = polar moment of inertia of the corss-section of the shaft
L = equivalent length of shaft

For this case

$$C = \frac{1.16 \times 10^6 \times 32.2 \times 12}{24.3}$$

$$= 1.848 \times 10^7 \ \frac{\text{lbs.ins.}^2}{\text{sec.}^2}$$

Now, for a two mass system

$$\text{Frequency constant } n = \frac{1}{2\pi}\sqrt{\frac{C\ I_p}{}\left\{\frac{1}{L_1} + \frac{1}{L_2}\right\}} \quad \text{/sec.}$$

$$= \frac{1}{2}\sqrt{1.848 \times 10^7\left\{\frac{1}{531} + \frac{1}{533}\right\}}$$

$$= 9.55\sqrt{6.97 \times 10^4} \quad \text{/mins.}$$

$$= \underline{2520} \quad \text{/min.}$$

If the system is considered as a three mass system, we have

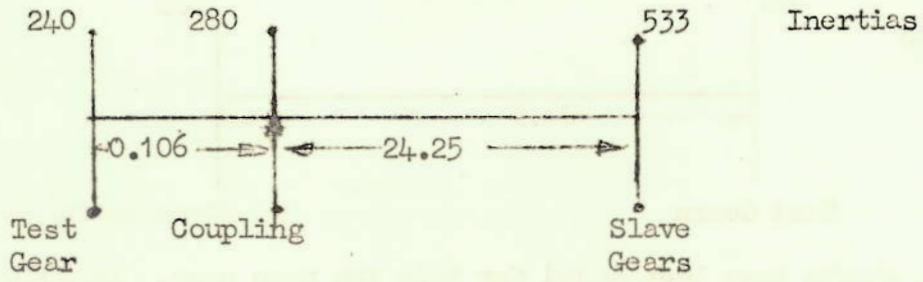

One third of the inertia of the smaller shaft has been added to each of the main inertias.

$$C_1 = \frac{1.16 \times 10^6 \times 32.2 \times 12}{0.106} = 4.23 \times 10^9 \quad \frac{\text{lbs.ins.}^2}{\text{sec.}^2}$$

$$C_2 = \frac{1.16 \times 10^6 \times 32.2 \times 12}{24.25} = 1.846 \times 10^7 \quad \frac{\text{lbs.ins.}^2}{\text{sec.}^2}$$

Now $a_1 = C_{1/\text{inertia}} = \frac{4.23 \times 10^9}{240} = 1.76 \times 10^7$

Similarly $b_1 = C_{1/\text{inertia}} \frac{4.23 \times 10^9}{280} = 1.51 \times 10^7$

$$a_2 = C_{2/\text{inertia}} \frac{1.846 \times 10^7}{280} = 6.6 \times 10^4$$

$$b_2 = C_{2/\text{inertia}} \frac{1.846 \times 10^7}{533} = 3.46 \times 10^4$$

Now Tuplin shows that

$$u^2 + (a_1 + b_1 + a_2 + b_2)\, u + (a_1 + b_1)(a_2 + b_2) - a_2 b_1 = 0$$

$$u^2 + 3.28 \times 10^7\, u + 3.27 \times 10^{12} - 10^{12} = 0$$

$$u^2 + 3.28 \times 10^7\, u + 2.27 \times 10^{12} = 0$$

Solving this in the usual way leads to :

$$u = \frac{-6.543 \times 10^7}{2} \text{ or } \frac{-1.70 \times 10^5}{2}$$

Subs $n^2 = -u$

and hence $n = 5720$ or 292 vibs/sec.
or 54600 or 2780 vibs/min.

If the case is now considered in which the two lines of shafting act together, a three mass system as shown below may be obtained. It is assumed here that any forcing of vibration comes from the test gears and none from the helical gears.

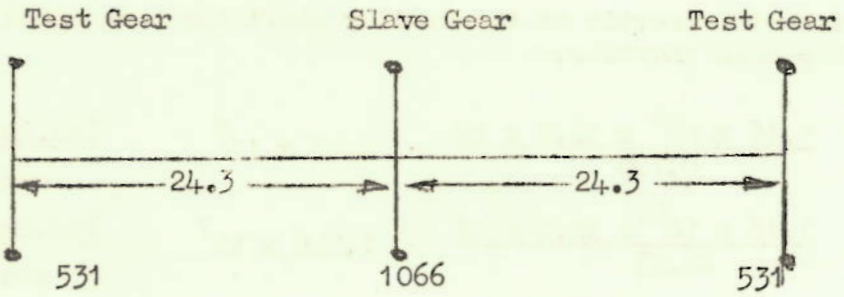

Inertias
lbs.ins^2

Spring constant for shaft = 1.848×10^7 lbs. ins.^{2}/sec.

$a_1 = b_1 = 3.48 \times 10^4$

$a_2 = b_2 = 1.735 \times 10^4$

Therefore $u^2 + 10.43 \times 10^4 u + (5.215^2 - 1.135^2)\ 10^8 = 0$

$u^2 + 10.43 \times 10^4 u + 24.2 \times 10^8 = 0$

This leads to $u = 3.48$ or -6.94×10^4

giving $n =$ 1790 or 2520 vibs/min.

If this last case is taken a step further by considering a five mass system, the configuration below is obtained :

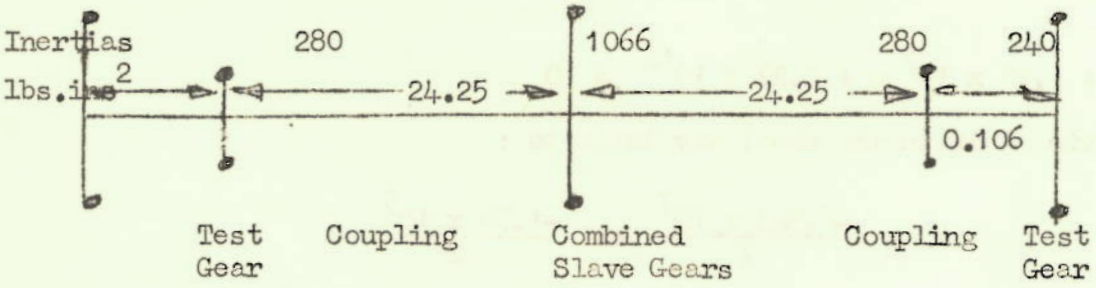

Considering one half of the system.
For an even mode vibration, we have the following configuration :

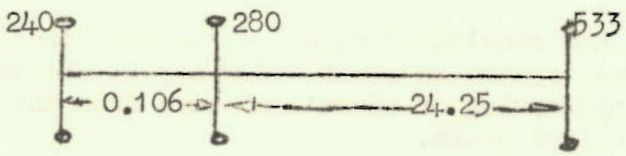

This system has been considered, giving frequencies of n = 54,600 or 2780 vibs/min. For an odd mode vibration

Inertias
lbs.ins^2

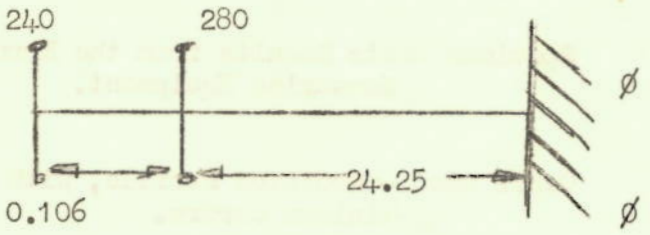

The central inertia is now infinite, and so $b_2 = 0$.

Therefore $u^2 + (a_1 + b_1 + a_2)\, u + (a_1 + b_1)\, a_2 b_1 = 0$

$$u^2 + 3.277 \times 10^7\, u + 2.155 \times 10^{12} - 9.98 \times 10^{11} = 0$$

$$u^2 + 3.277 \times 10^7\, u + 1.157 \times 10^{12} = 0$$

Giving $u = -3.27 \times 10^7$ or 6.9×10^4

$\therefore$ n = 54,700 or 2,500 vib/min.

It would appear that the first and second and the third and fourth natural vibrations are close together. From consideration of the above cases, it appears that the modes of vibration are as follows :-

1st mode	1,790 vibs/min.
2nd mode	2,520 vibs/min.
3rd mode	54,600 vibs/min.
4th mode	54,700 vibs/min.

APPENDIX 3

Dynamic Load on Spur Gear Teeth.

Specimen Tests Results from the Error Measuring Equipment.

Gears Used - Modified Profile, with minimum errors.

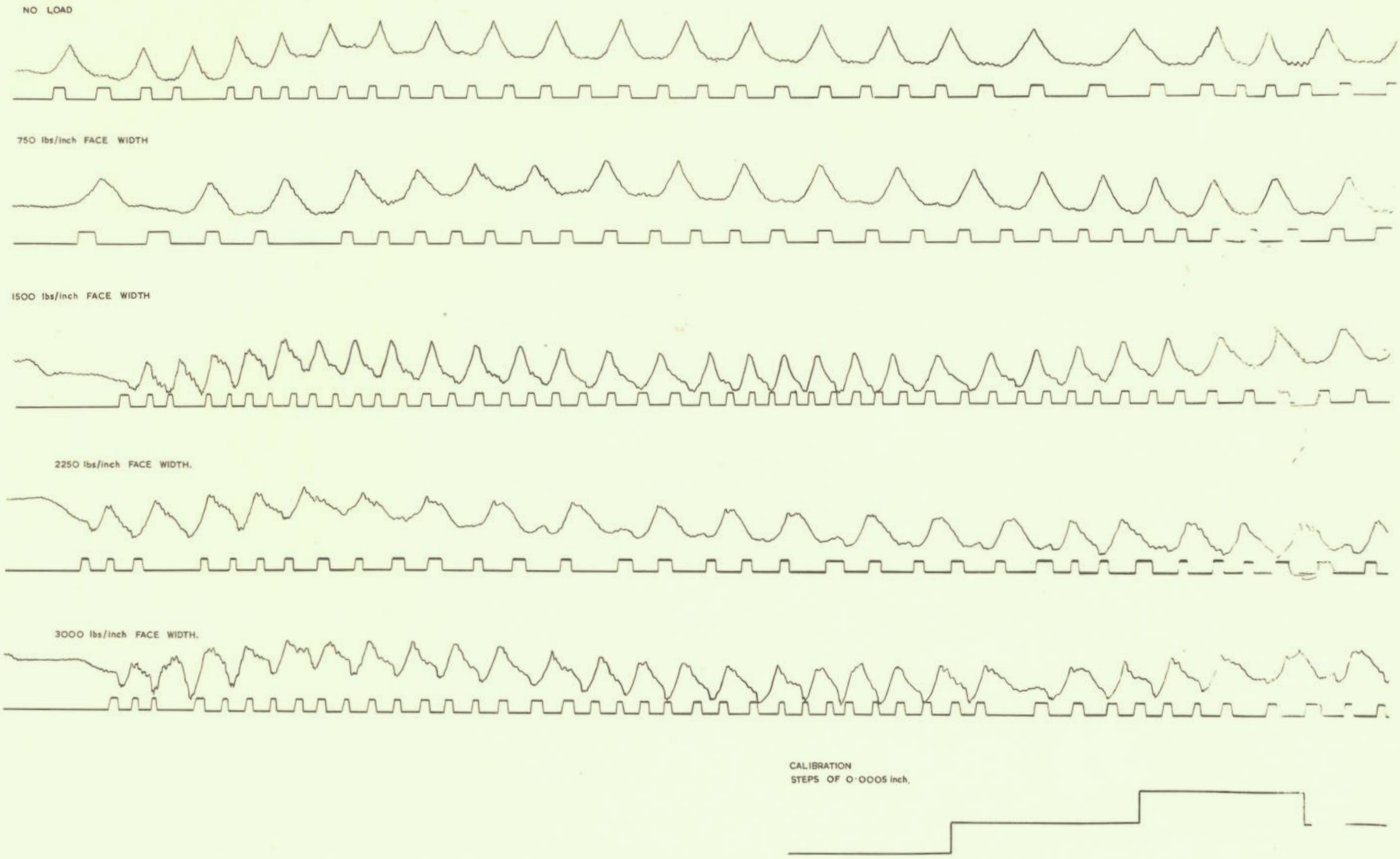
NO LOAD
750 lbs/inch FACE WIDTH
1500 lbs/inch FACE WIDTH
2250 lbs/inch FACE WIDTH.
3000 lbs/inch FACE WIDTH.
CALIBRATION
STEPS OF 0·0005 inch.

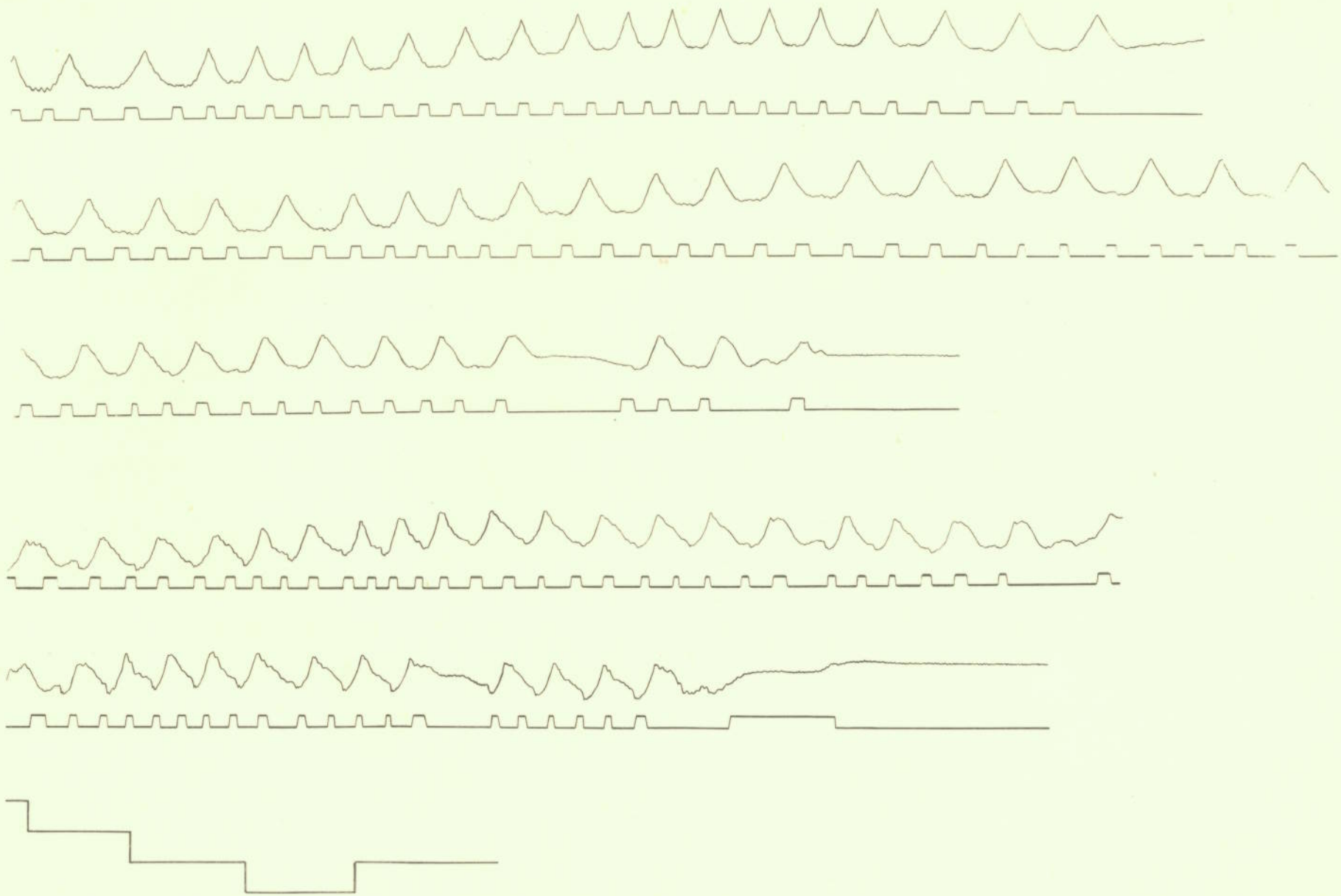

TABLE I. Showing Controlled Errors manufactured in Test Gears

Gear Identification No.	Profile	Spacing on one Pressure Side			
1/1	Modified to Normal R.R. Practice	Pitches	36/1	- 8/9	- .0008 in. greater than nominal
		"	9/10	- 17/18	- nominal
		"	18/19	- 26/27	- .0011 in. less than nominal
2/1	Pure involute	"	27/28	- 35/36	- .0003 in. greater than nominal
1/2	Modified to Normal R.R. Practice	Pitch	36/1		- .0005 greater than nominal
		Pitches	1/2	- 8/9 incl.	- nominal
		Pitch	9/10		- .0008 less than nominal
		Pitches	10/11	- 17/18 incl.	- nominal
		Pitch	18/19		- .0011 less than nominal
2/2	Pure involute	Pitches	19/20	- 26/27 incl.	- nominal
		Pitch	27/28		- .0014 greater than nominal
		Pitches	28/29	- 35/36	- nominal

Gear Teeth Numbere 1 - 36

Nominal Tooth Spacing on other pressure side of all gears.

TABLE II. Showing Type and Magnitude of Errors available for investigation with Test Gears.

Profile	Driver Gear No.	Driver Gear Tooth Spacing	Driven Gear No.	Driven Gear Tooth Spacing	Controlled Errors Available for Investigation
Modified or Pure Involute	1/2 or 2/2	Nominal	1/1 or 2/1	Nominal	Nil
Modified or Pure Involute	1/2 or 2/2	Nominal	1/1 or 2/1	Constant Errors	+ .0005 in. change - .0008 in. " - .0011 in. " + .0014 in. "
Modified or Pure Involute	1/1 or 2/1	Constant Errors	1/2 or 2/2	Nominal	- .0005 in. change + .0008 in. " + .0011 in. " - .0005 in. "
Modified or Pure Involute	1/1 or 2/1	Nominal	1/2 or 2/2	Isolated Errors	+ .0005 in. - .0008 in. - .0011 in. + .0014 in.

TABLE 3. Individual tooth errors. (Determined at Rolls-Royce)

Gear No.	IS.1556/52 A 1/1				IS.1556/52 A 1/2				IS.1556/53 2/1				IS.1556/53 2/2			
	1st Side		2nd Side		1st Side		2nd Side		1st Side		2nd Side		1st Side		2nd Side	
Tooth Space Number	Pitch Difference from Equal Spacing															
	Target	Actual	Target	Actual	Target	Actual	Target	Actual	Target	Actual	Target	Actual	Target	Actual	Target	Actual
36-1	+.0008	+.0006		-.000025	+.0005	+.0006		-.000075	+.0008	+.0009		-.00025	+.0005	+.0005		-.00015
1-2	"	+.000925		+.0001	.00000	+.00005		+.000025	"	+.0010		-.000275	.00000	+.0001		+.00005
2-3	"	+.000825		+.000025	"	.00000		.00000	"	+.0008		+.000125	"	-.0001		+.0001
3-4	"	+.0007		+.0001	"	.00000		.00000	"	+.000925		-.000175	"	+.00015		-.00015
4-5	"	+.00095		+.00005	"	.00000		+.00005	"	+.000825		.00000	"	+.0002		-.0001
5-6	"	+.000925		+.000025	"	.00000		-.000125	"	+.00075		-.00005	"	.00000		-.00005
6-7	"	+.0008		.00000	"	.00000		-.000025	"	+.000975		-.00015	"	+.00005		.00000
7-8	"	+.0010		.0000	"	-.000075		.00000	"	+.000825		-.0001	"	+.00005		.00000
8-9	"	+.001025		+.000075	"	-.000075		.00000	"	+.0010		.00000	"	.00000		-.00005
9-10	.0000	-.00006		.00000	-.0008	-.000925		-.00015	.00000	-.000025		-.000075	-.0008	-.00075		-.0001
10-11	"	+.00005		-.00005	.00000	-.00005		-.0001	"	.00000		+.000025	.00000	-.00005		.00000
11-12	"	-.000025		.00000	"	.00000		.00000	"	.00000		+.000075	"	+.0001		+.00005
12-13	"	-.000175		.00000	"	+.000025		-.000025	"	-.00005		-.000025	"	-.0001		.00000
13-14	"	.0000		-.000175	"	-.000075		-.000075	"	-.000075		.00000	"	-.000025		+.00005
14-15	"	.0000		-.000025	"	-.000075		-.0001	"	.00000		+.00015	"	-.000175		.00000
15-16	"	-.000325	FLANKS	-.000075	"	+.00015	FLANKS	-.000025	"	-.001	FLANKS	.00000	"	-.000175	FLANKS	+.0001
16-17	"	-.000175		-.000075	"	-.000025		-.00005	"	-.000125		.00000	"	.00000		+.0001
17-18	"	-.00025		.00000	"	-.000125		.00000	"	+.0001		+.0001	"	-.000025		-.00005

PHOTOGRAPHS

No. 1. General view of the test rig

2. General view of the test gears

3. General view of the slave gears

4. The capacity pick-up

5. Strain gauge beam attached to a gear tooth

6. The position of the lead zirconate crystals

7. The general view of the Error-Measuring Equipment

8. The Error-Measuring Equipment with the Magna Gauge in position

9. The Error-Measuring device with clock gauge in position

10. The rig showing the loading coupling, etc.

11. Photo-Electric Transducers

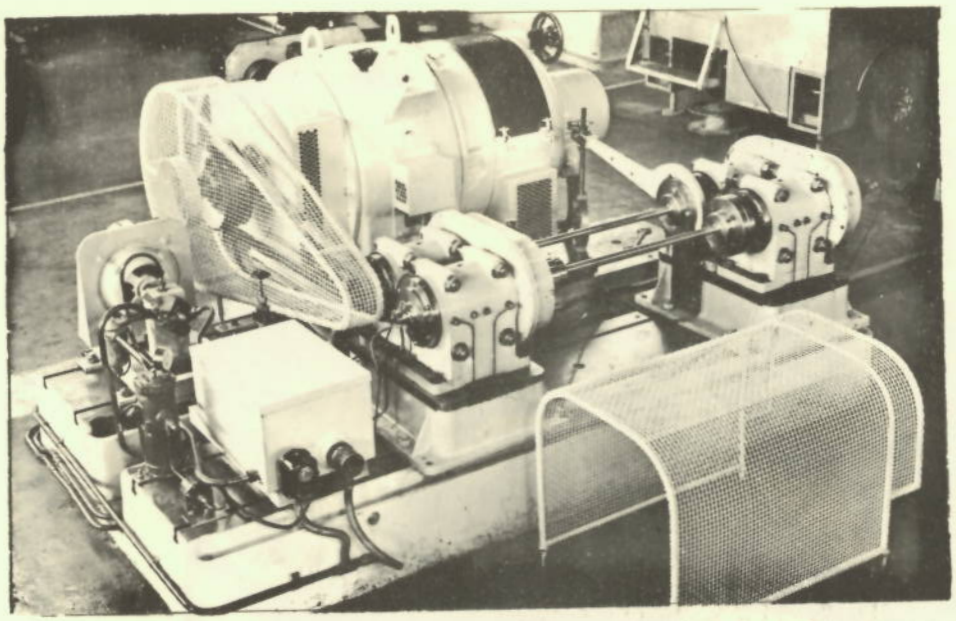

PHOTOGRAPH NO. 1.

PHOTOGRAPH SHOWING GENERAL VIEW
OF THE GEAR TEST RIG.

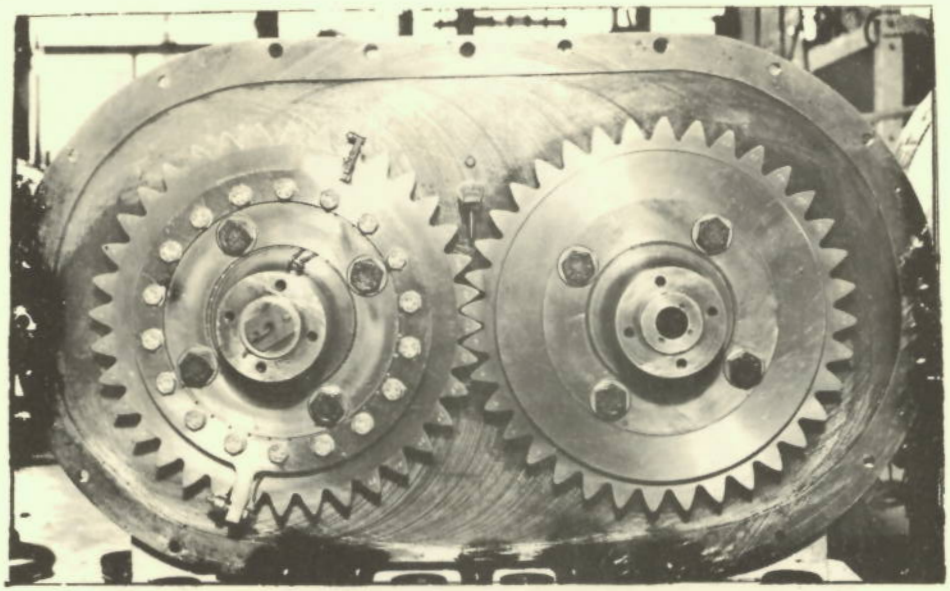

PHOTOGRAPH NO. 2.

PHOTOGRAPH SHOWING GENERAL VIEW
OF TEST GEARS (MODIFIED PROFILE.)

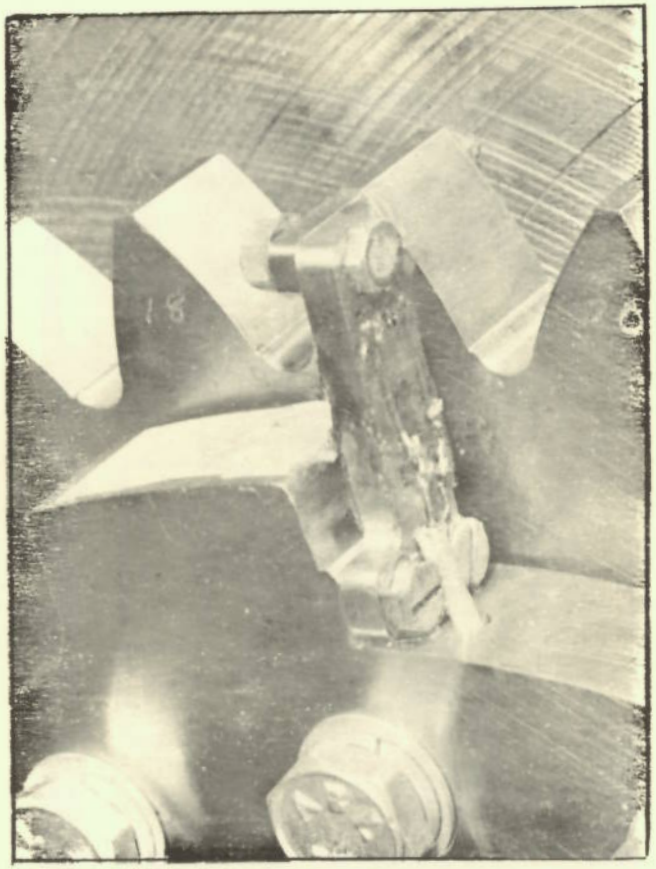

PHOTOGRAPH NO. 5.

PHOTOGRAPH SHOWING STRAIN GAUGE BEAM ATTACHED TO GEAR TOOTH

PHOTOGRAPH NO. 6.

PHOTOGRAPH SHOWING POSITION OF LEAD ZIRCONATE CRYSTALS (ONE ON FAR SIDE OF BEAM)

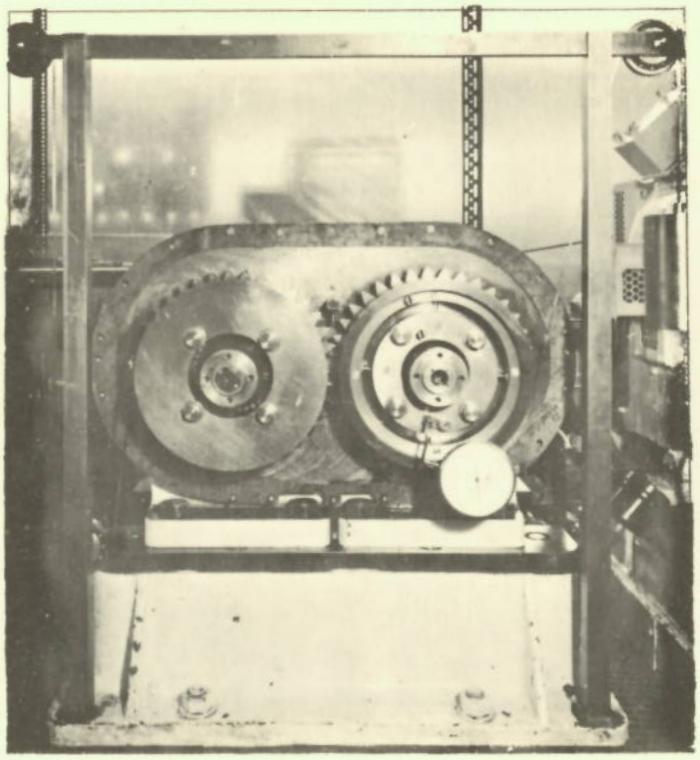

PHOTOGRAPH NO. 7.
PHOTOGRAPH SHOWING GENERAL VIEW OF THE
'ERROR MEASURING EQUIPMENT'

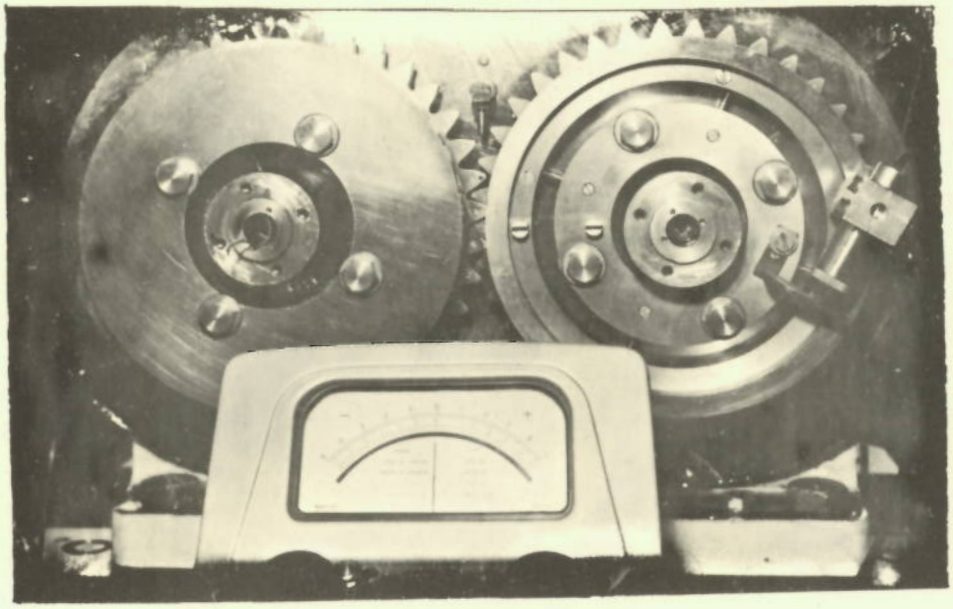

PHOTOGRAPH NO. 8.
PHOTOGRAPH OF THE 'ERROR MEASURING DEVICE'
WITH THE MAGNA GAUGE IN POSITION

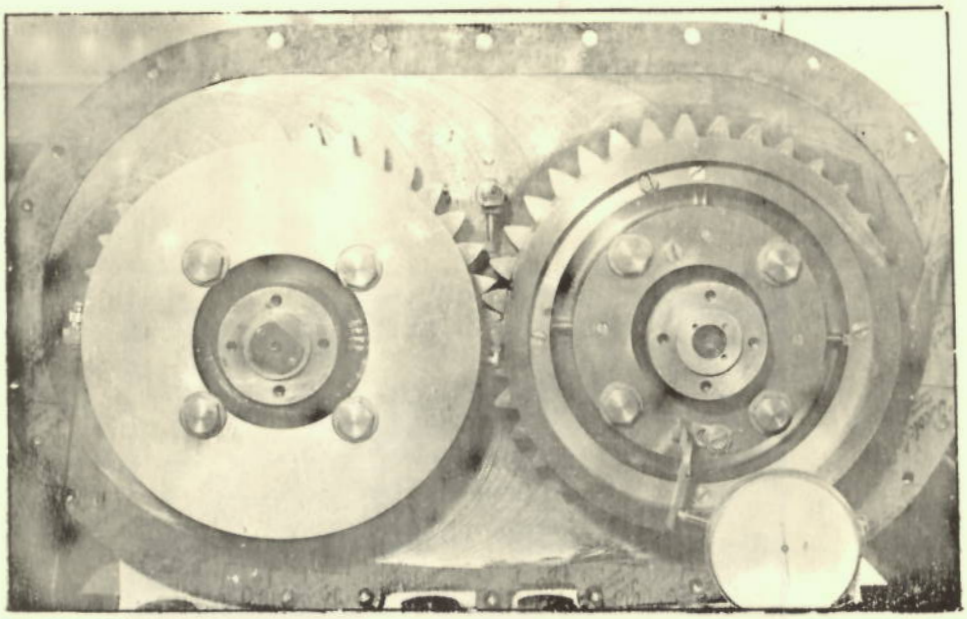

PHOTOGRAPH NO. 9.

PHOTOGRAPH OF THE 'ERROR MEASURING DEVICE' WITH CLOCK GAUGE IN POSITION

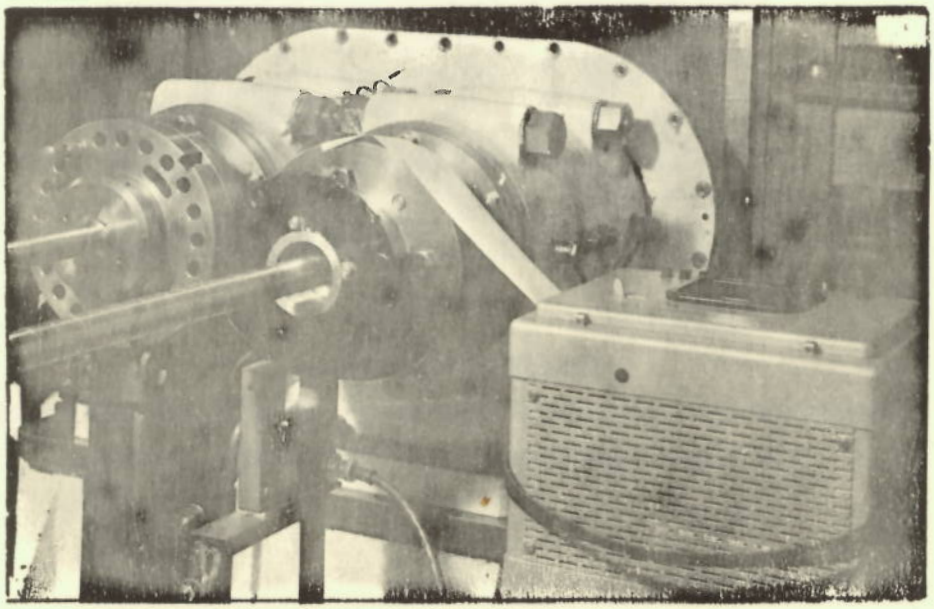

PHOTOGRAPH NO. 10.

PHOTOGRAPH OF RIG SHOWING LOADING COUPLING, PHOTO CELL AND DISC FOR MEASURING SPEED, AND RECORDER USED INITIALLY FOR RECORDING TRANSMISSION ERRORS.

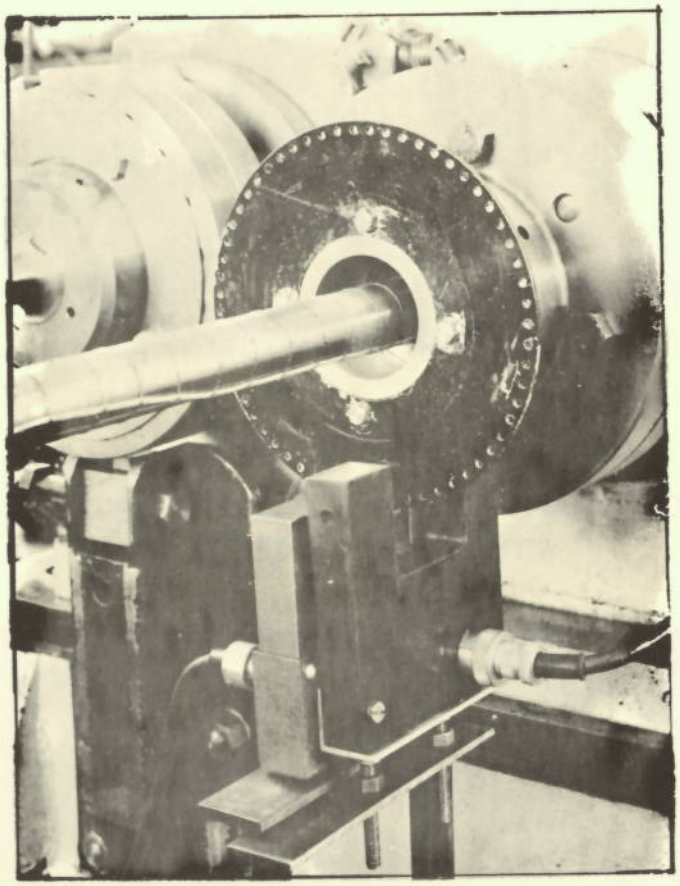

PHOTOGRAPH NO. 11.

PHOTOGRAPH SHOWING PHOTO-ELECTRIC TRANSDUCERS FOR SHAFT-SPEED AND TRIGGERING SIGNAL.

FIGURES

1. Diagrammatic Arrangement of Test Rig
2. Typical Bearing Arrangement
3. Block diagram of 1st Electronic Timer for Gear Test Rig
4. Block diagram of 2nd Electronic Timer for Gear Test Rig
5. Circuit diagram of 1st Electronic Timer
6. Circuit diagram of 2nd Electronic Timer
7. Capacity Pick up
8. Principle of the Capacity Slip Ring
9. Principle of the Grid-dip system
10. Block diagram showing instrumentation employed on the gear rig

11 - 29 incl. Test Results

(i) Specimen results using the Capacity Pick-Up and the Grid-dip Oscillator

(ii) Specimen results using the Capacity Pick-Up and the Capacity Transmitter

(iii) Specimen results using the Lead Zirconate Crystal and the Mercury Slip Ring. (Crystal cemented to the side of tooth).

In all the above tests the following conditions were standardised.

Oil	Castrol Hypoy 90
Oil temperature	60°C.
Oil pressure	30 lbs/sq.inch
Oil flow	22 gallons/hour

30 - 37 incl. Maag Profile Diagrams for the test gears

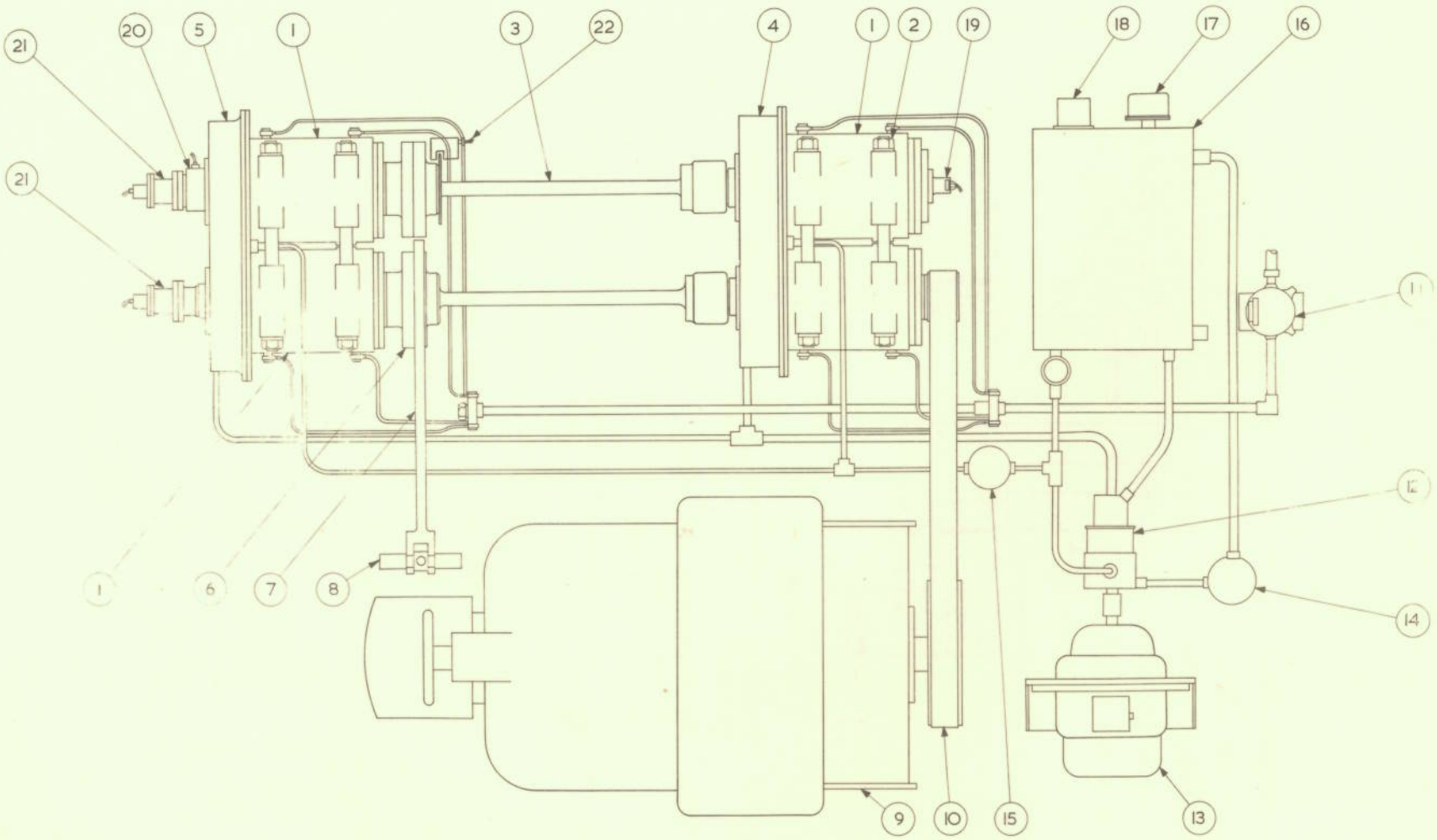

FIG. I. DIAGRAMMATIC ARRANGEMENT OF TEST RIG.

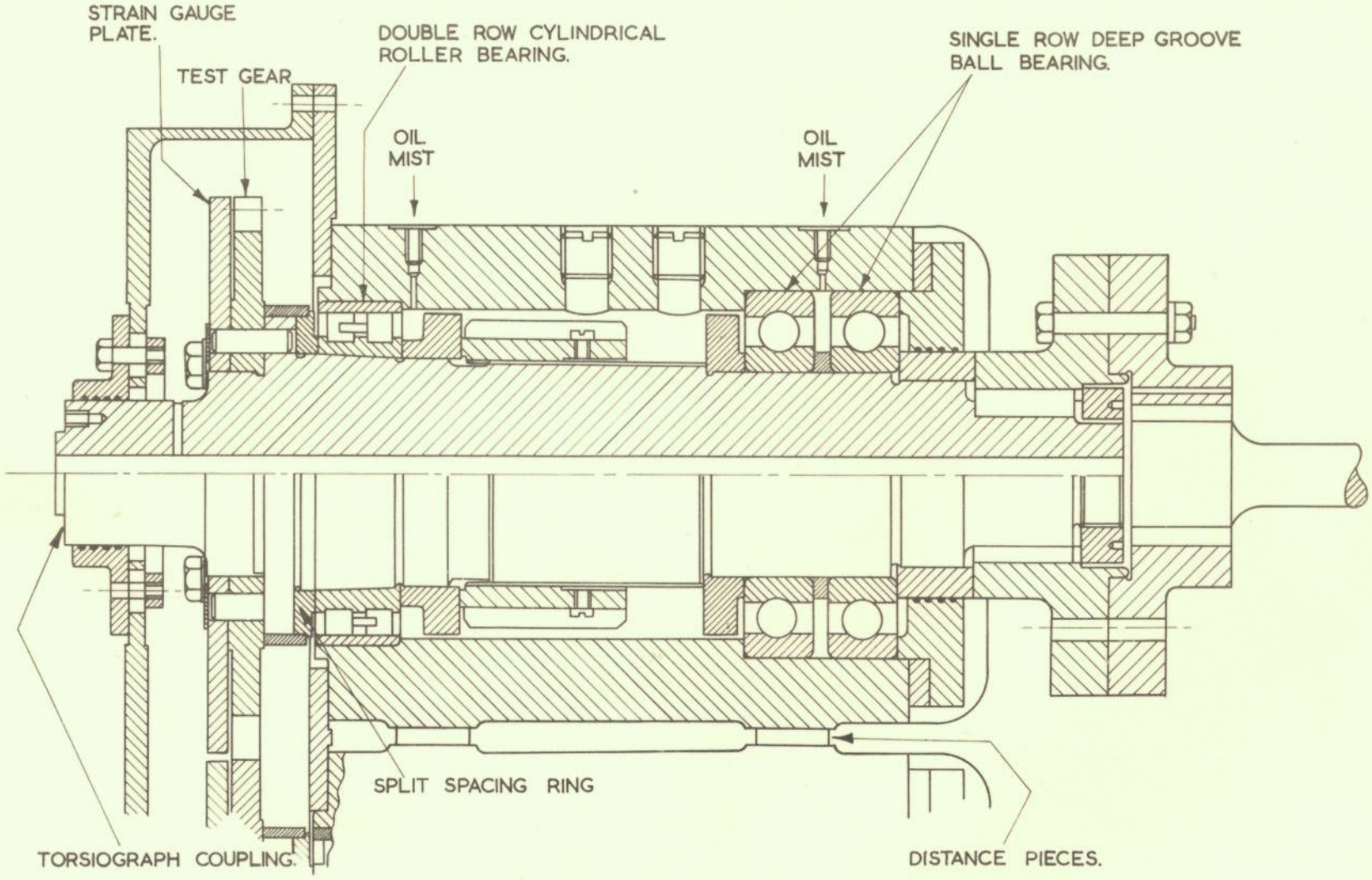

FIG. 2. TYPICAL BEARING ARRANGEMENT

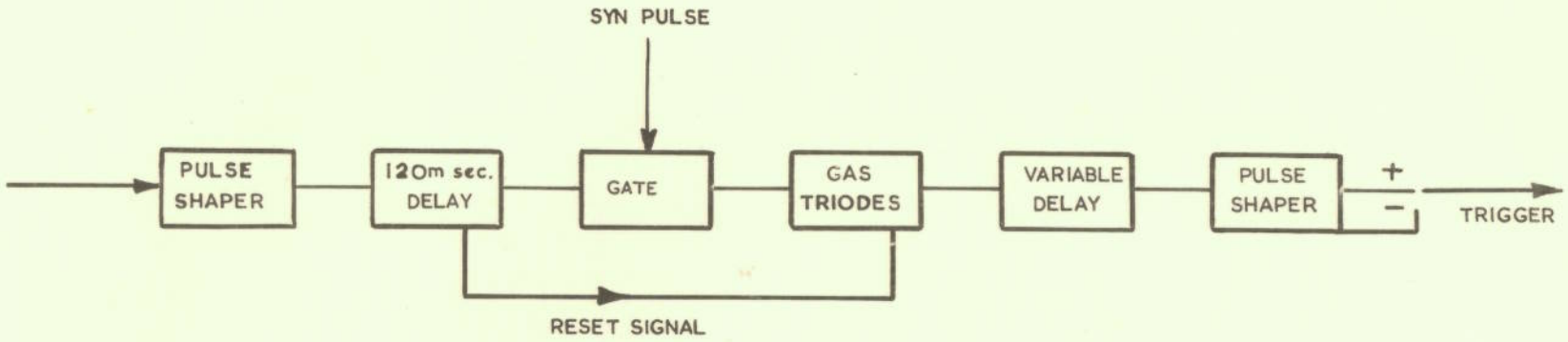

FIG. 3. DIAGRAM OF 1st ELECTRONIC TIMER FOR THE GEAR TEST RIG.

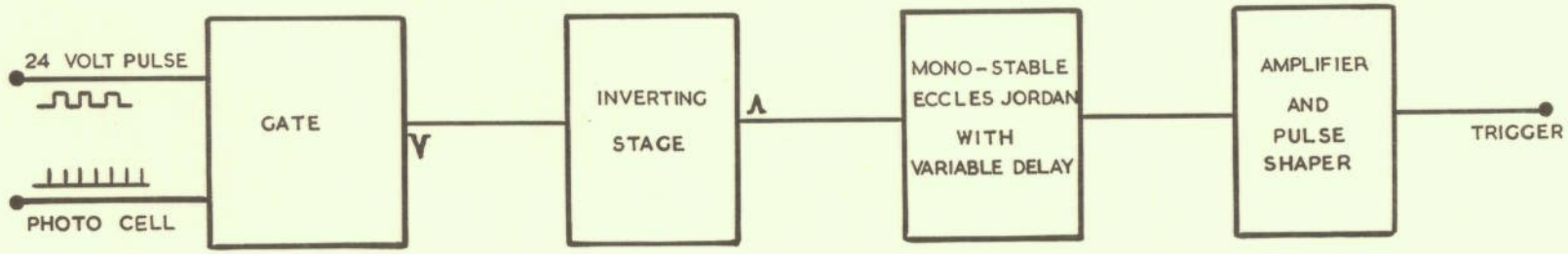

FIG. 4. BLOCK DIAGRAM OF 2nd ELECTRONIC TIME FOR GEAR TEST RIG.

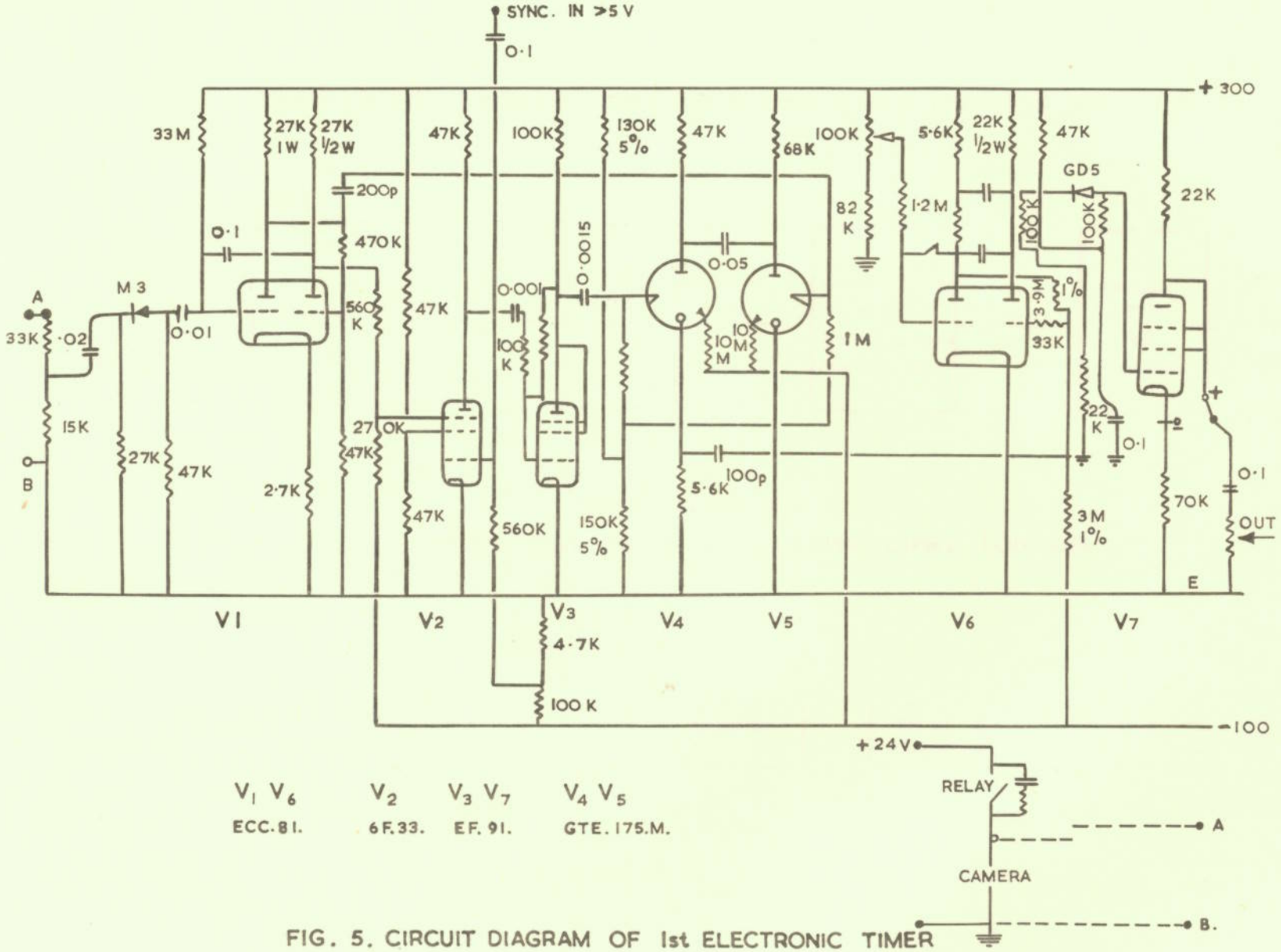

V_1 V_6 ECC. 81. V_2 6F. 33. V_3 V_7 EF. 91. V_4 V_5 GTE. 175.M.

FIG. 5. CIRCUIT DIAGRAM OF 1st ELECTRONIC TIMER

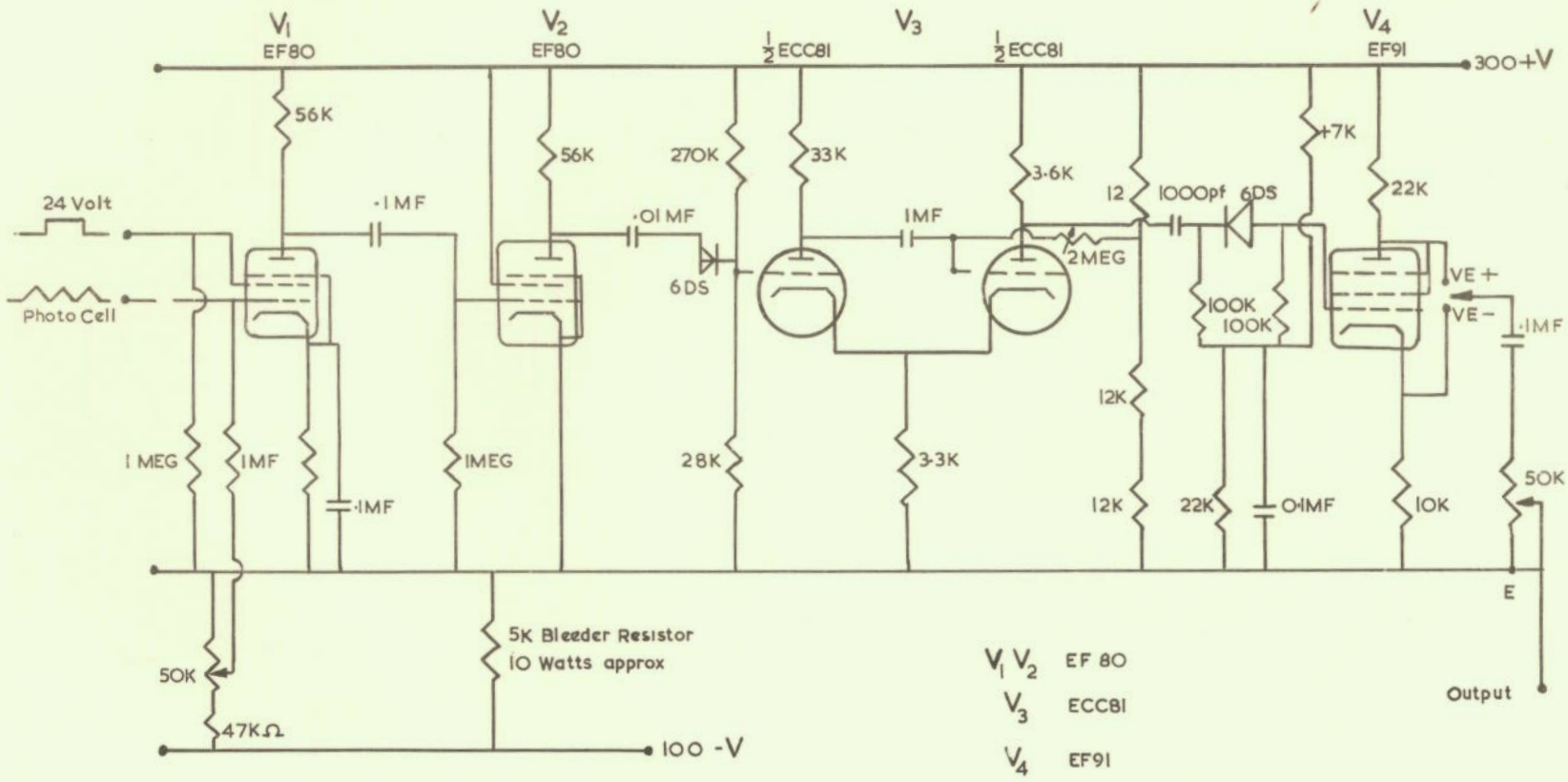

FIG. 6. CIRCUIT DIAGRAM OF 2nd ELECTRONIC TIMER

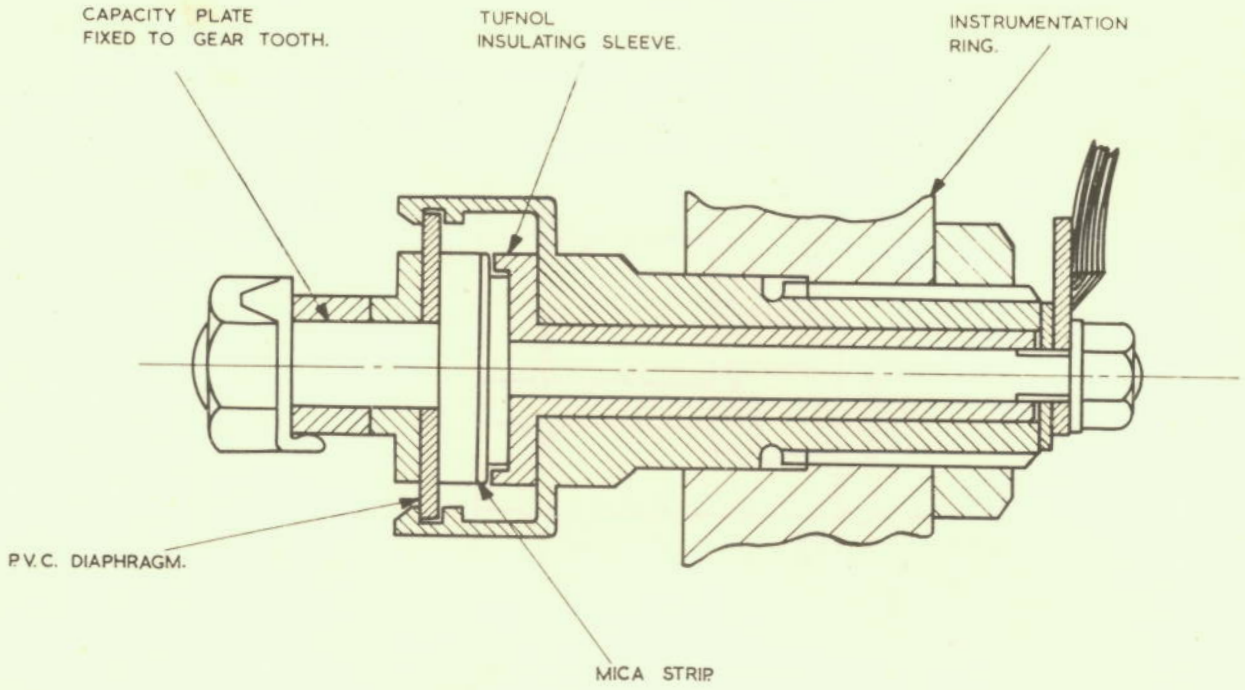

FIG. 7. CAPACITY PICK – UP.

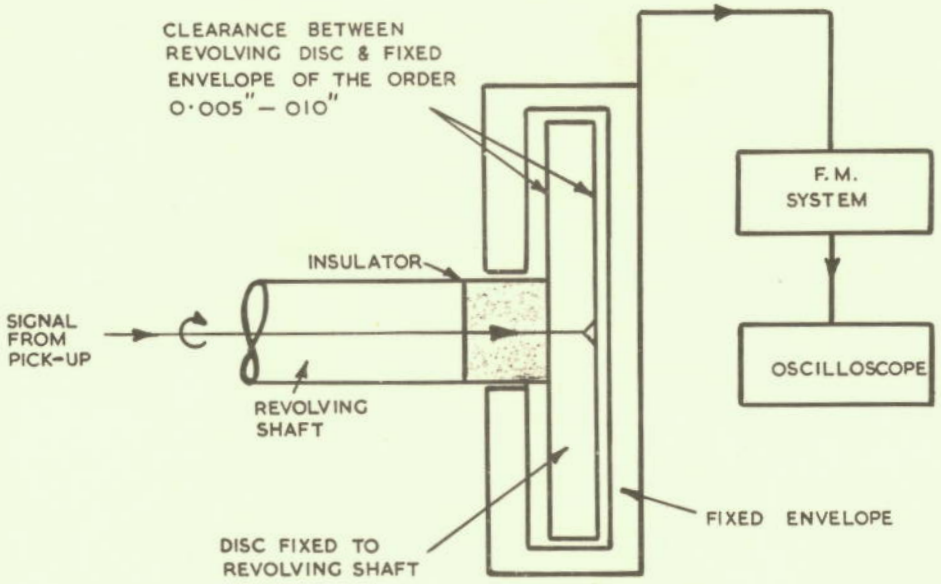

FIG. 8 PRINCIPLE OF THE CAPACITY SLIP RING.

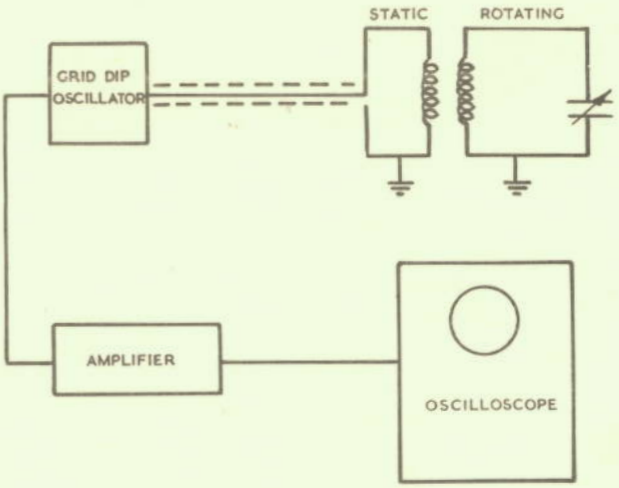

FIG. 9. GRID DIP SYSTEM FOR MEASURING CHANGES OF CAPACITY

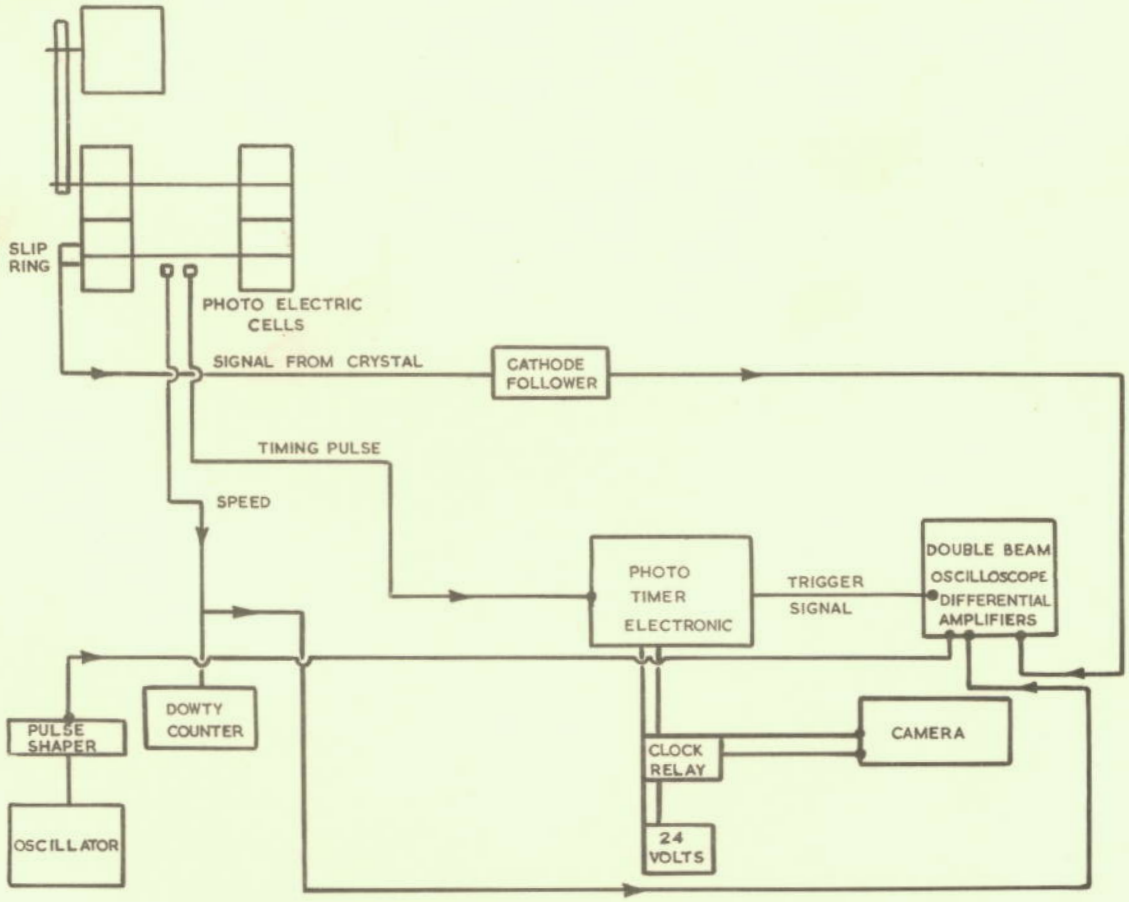

FIG. 10. BLOCK DIAGRAM SHOWING INSTRUMENTATION EMPLOYED ON GEAR RIG.

RESULTS OF TESTS USING THE CAPACITY PICK-UP AND THE GRID-DIP OSCILLATOR
GAIN X 10

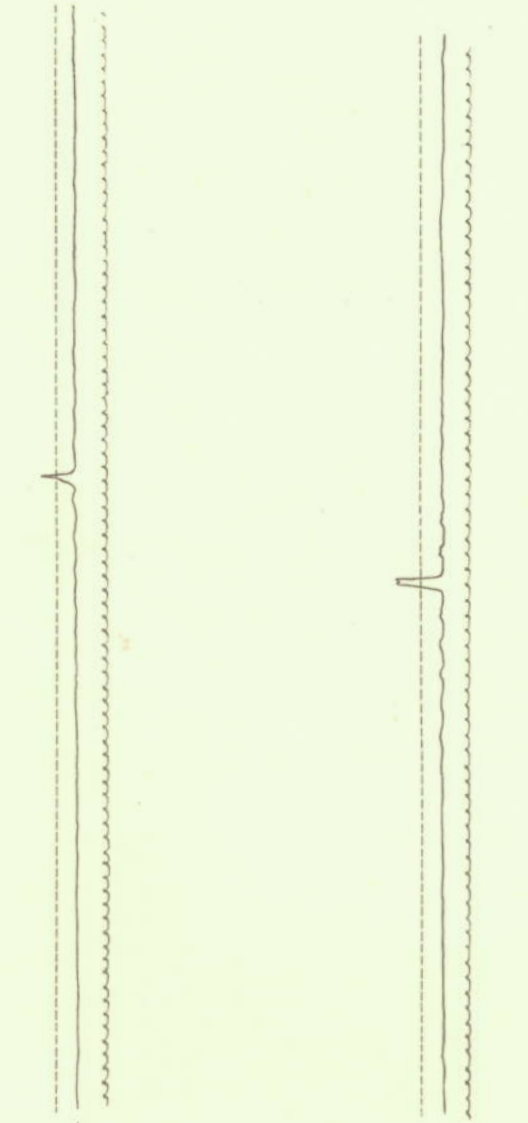

FIG. II. LOAD 1119 LBS / INCH FACE WIDTH

JLTS OF TESTS USING THE CAPACITY PICK-UP AND THE CAPACITY TRANSMITTER

GAIN (X 155)

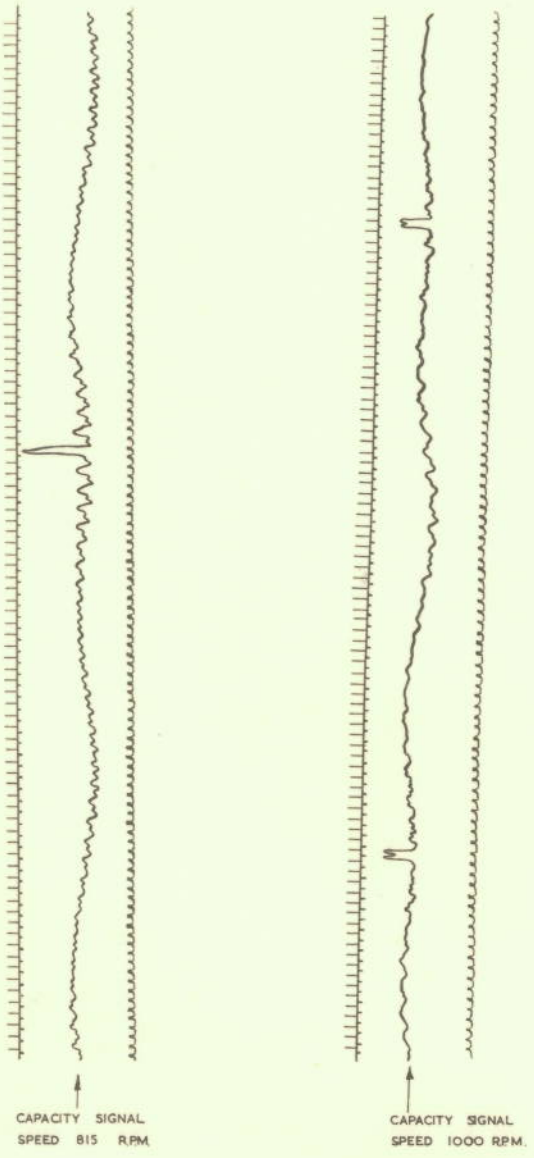

FIG. 12. LOAD 750 LBS / INCH FACE WIDTH

GAIN (X 155)

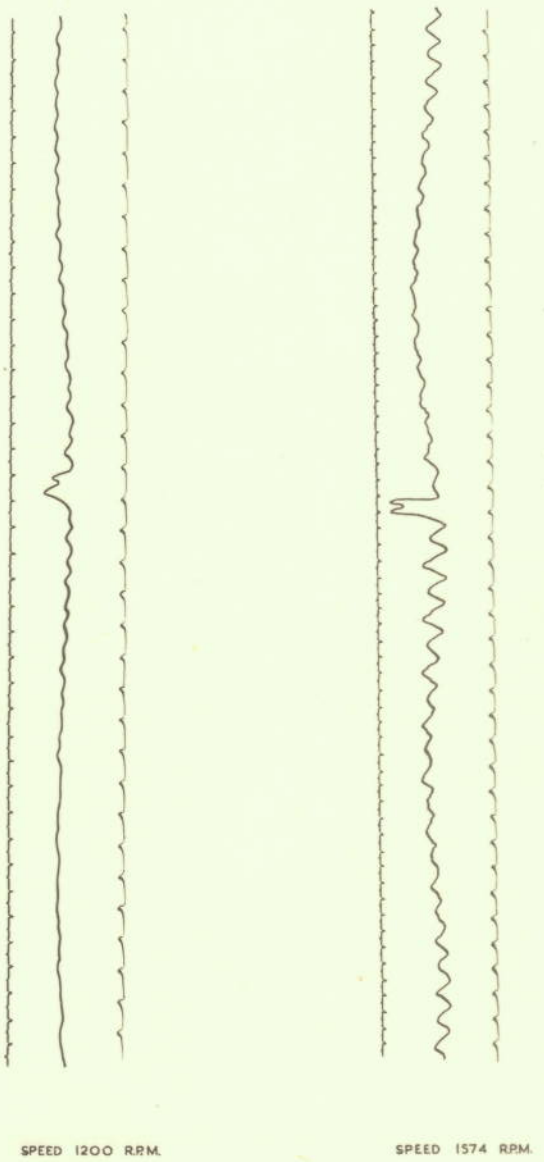

FIG. 13. LOAD 750 LBS. / INCH FACE WIDTH

GAIN (X 155)

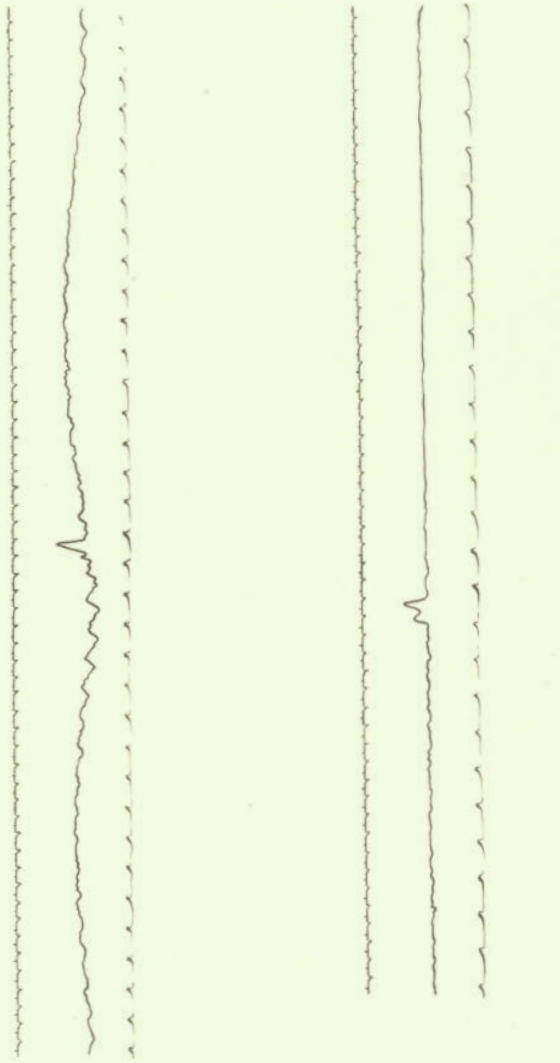

SPEED 1765 R.P.M.

SPEED 2008 R.P.M.

FIG. 14. LOAD 750 LBS. / INCH FACE WIDTH

GAIN (X 155)

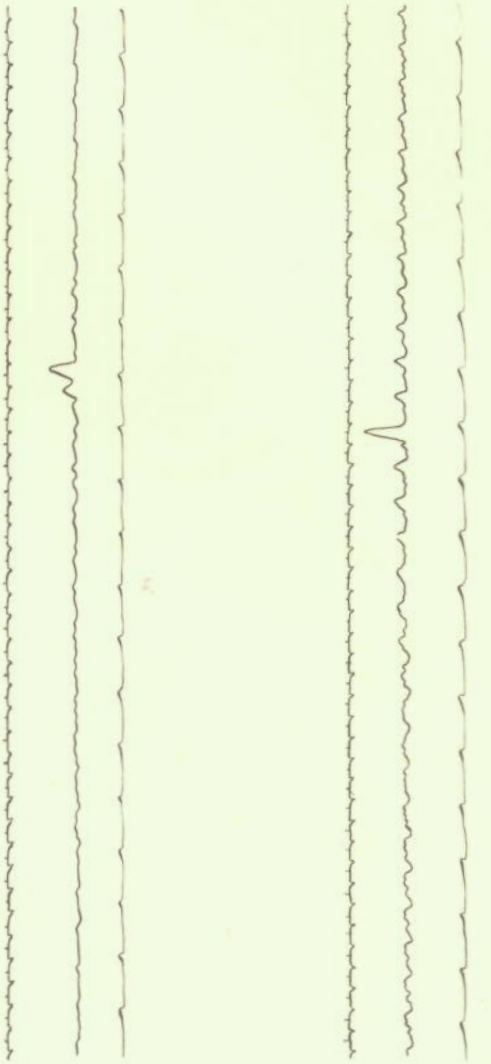

SPEED 2302 R.P.M.

SPEED 2601 R.P.M.

FIG. 15. LOAD 750 LBS / INCH FACE WIDTH

GAIN (X 155)

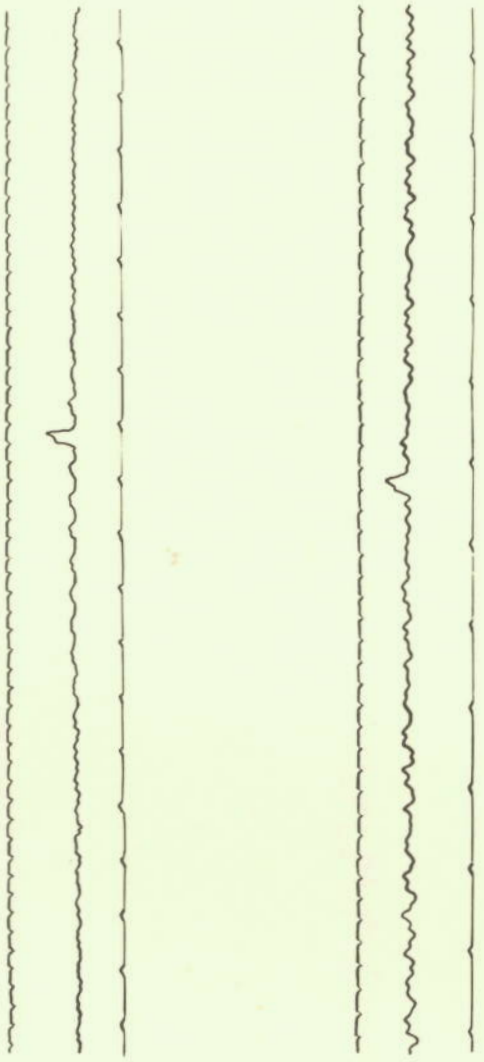

SPEED 2905 R.P.M.

SPEED 3759 R.P.M.

FIG. 16. LOAD 750 LBS / INCH FACE WIDTH

GAIN (X 155)

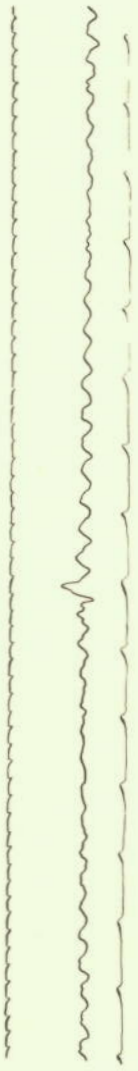

SPEED 4000 R.P.M.

FIG. 17. LOAD 750 LBS / INCH FACE WIDTH

TESTS USING LEAD ZIRCONATE CRYSTAL CEMENTED TO SIDE OF TOOTH AND SIGNAL TRANSMITTED BY MEANS OF A MERCURY SLIP-RING
LOAD 3,000 LBS / INCH FACE WIDTH

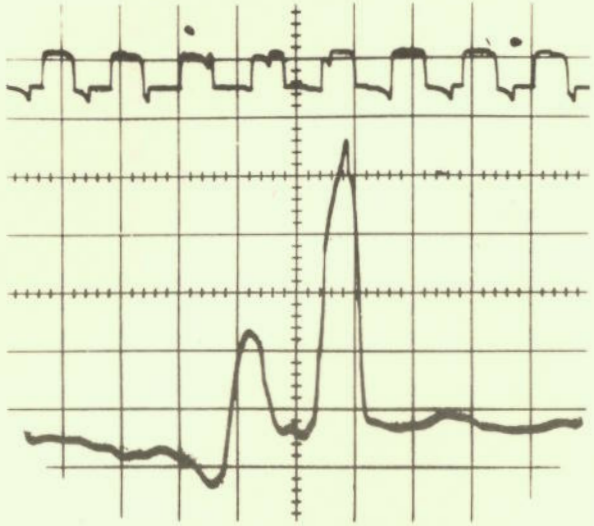

SPEED 814 R.P.M. LOAD 3,000 LBS/INCH FACE WIDTH. SENSITIVITY 1 VOLT/CMS
HORIZONTAL SWEEP MAGNIFICATION X 5 TIME BASE 5 MILLISEC/CMS

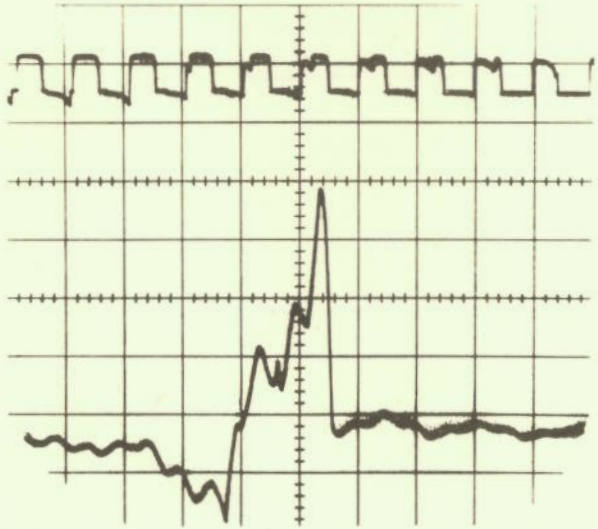

SPEED 1002 R.P.M. LOAD 3,000 LBS/INCH FACE WIDTH. SENSITIVITY 1 VOLT/CMS
HORIZONTAL SWEEP MAGNIFICATION X 5 TIME BASE 5 MILLISEC/CMS

FIG. 18

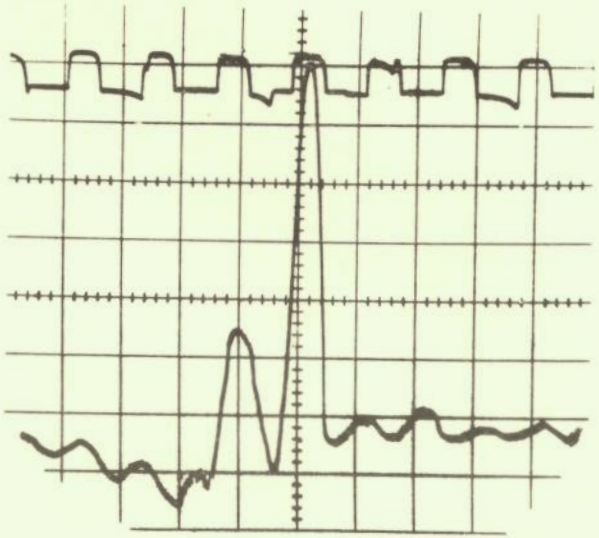

SPEED 1540 R.P.M. LOAD 3,000 LBS/INCH FACE WIDTH. SENSITIVITY 1 VOLT/CMS
HOPIZONTAL SWEEP MAGNIFICATION X 10 TIME BASE 5 MILLYSEC/CMS

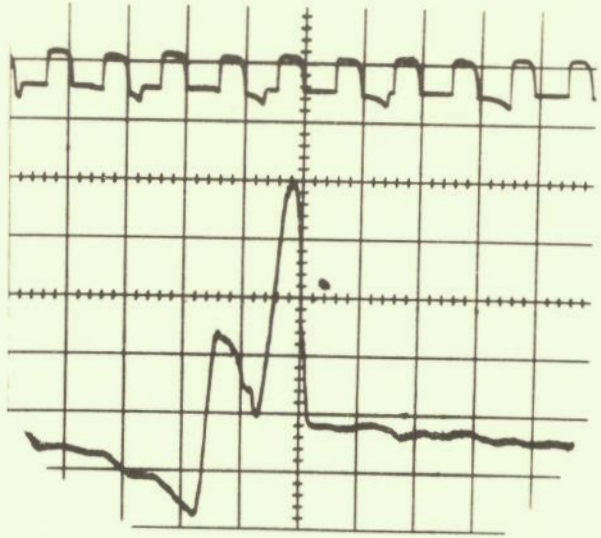

SPEED 2000 R.P.M. LOAD 3,000 LBS/INCH FACE WIDTH. SENSITIVITY 1 VOLT/CMS
HORIZONTAL SWEEP MAGNIFICATION X 10 TIME BASE 5 MILLISEC/CMS

FIG 19

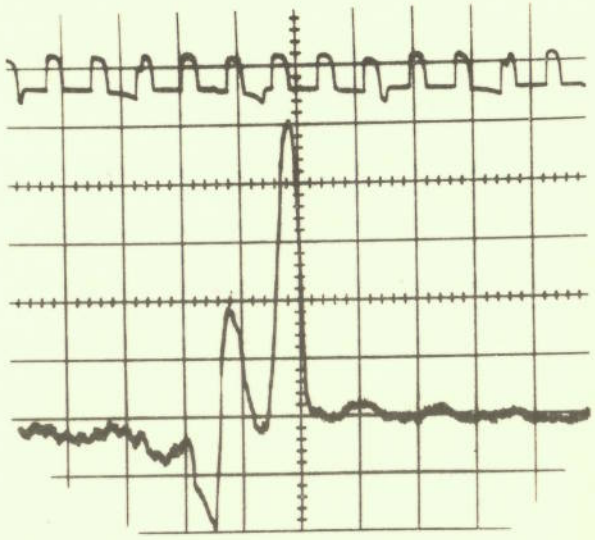

SPEED 2529 R.P.M. LOAD 3,000 LBS/INCH FACE WIDTH. SENSITIVITY 1 VOLT/CMS
HORIZONTAL SWEEP MAGNIFICATION X 10 TIME BASE 5 MILLISEC /CMS

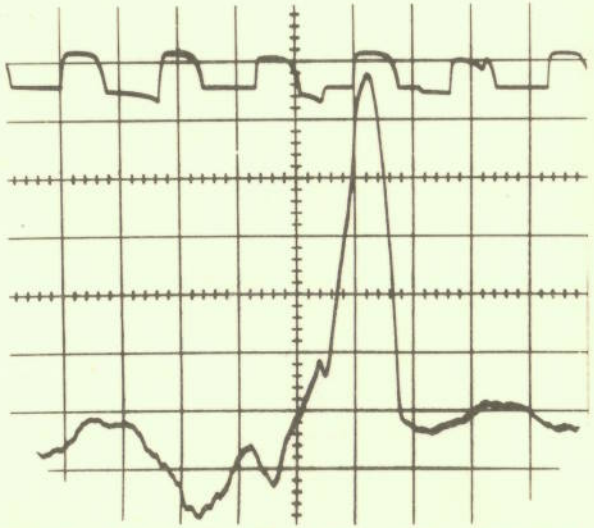

SPEED 3010 R.P.M. LOAD 3,000 LBS/INCH FACE WIDTH. SENSITIVITY 1 VOLT /CMS
HORIZONTAL SWEEP MAGNIFICATION X 10 TIME BASE 2 MILLISEC/CMS

FIG 20

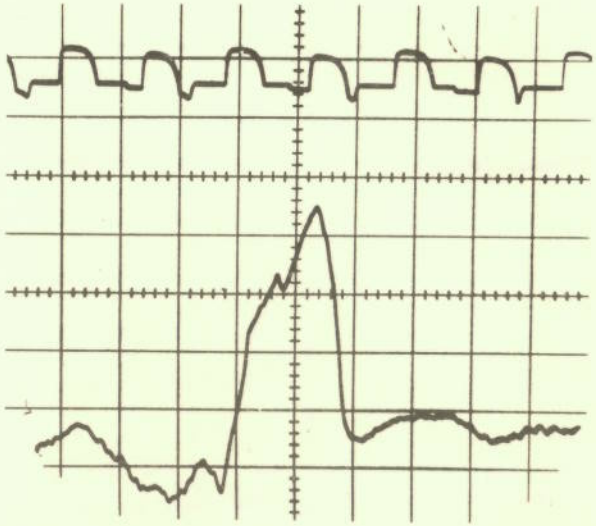

SPEED 3499 R.P.M. LOAD 3,000 LBS/INCH FACE WIDTH. SENSITIVITY 1 VOLT /CMS
HORIZONTAL SWEEP MAGNIFICATION X 10 TIME BASE 2 MILLISEC / CMS

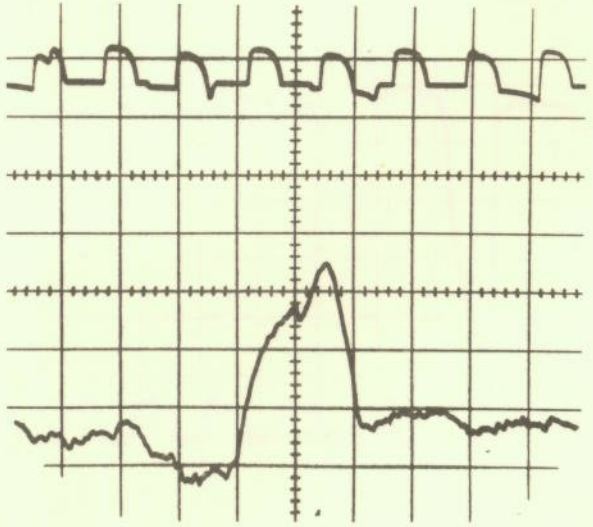

SPEED 4040 R.P.M. LOAD 3,000 LBS/INCH FACE WIDTH. SENSITIVITY 1 VOLT/CMS
HORIZONTAL SWEEP MAGNIFICATION X 10 TIME BASE 2 MILLISEC /CMS

FIG. 21

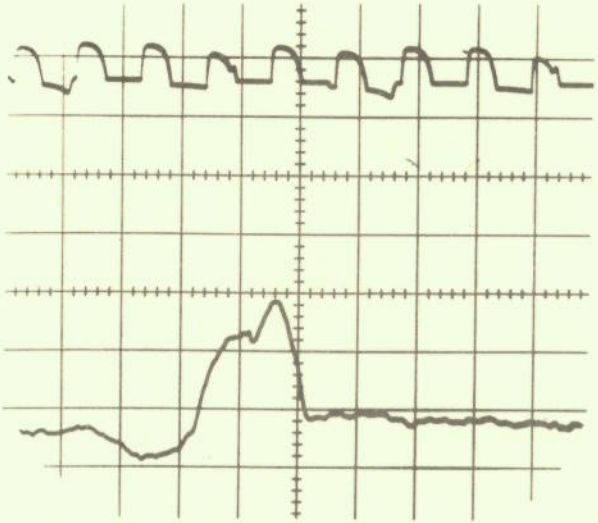

SPEED 4524 R.P.M. LOAD 3,000 LBS / INCH FACE WIDTH. SENSITIVITY 1 VOLT/CMS
HORIZONTAL SWEEP MAGNIFICATION X 10 TIME BASE 2 MILLISEC /CMS

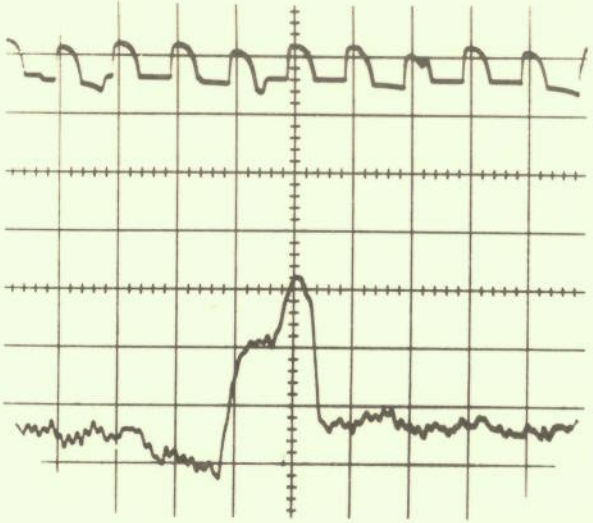

SPEED 5000 R.P.M. LOAD 3,000 LBS /INCH FACE WIDTH. SENSITIVITY 1 VOLT /CMS
HORIZONTAL SWEEP MAGNIFICATION X 10 TIME BASE 2 MILLISEC/CMS

FIG 22

TESTS USING LEAD ZIRCONATE CRYSTAL CEMENTED TO SIDE OF TOOTH
AND SIGNAL TRANSMITTED BY MEANS OF A MERCURY SLIP — RING
LOAD 1500 LBS / INCH FACE WIDTH
(HALF LOAD)

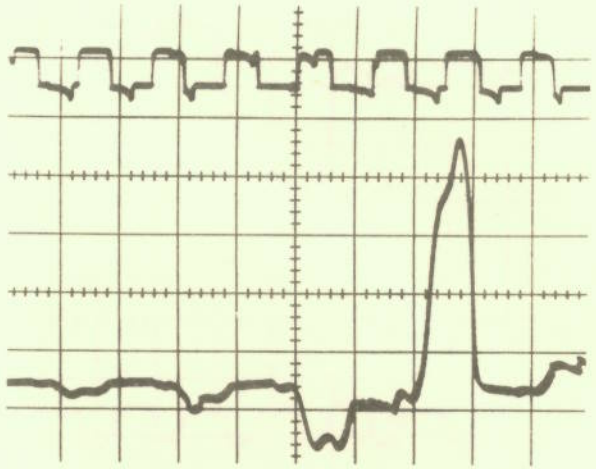

SPEED 764 R.P.M. LOAD 1500 LBS/INCH FACE WIDTH SENSITIVITY 2 VOLTS/CMS
HORIZONTAL SWEEP MAGNIFICATION X 5 TIME BASE 5 MILLISEC / CMS

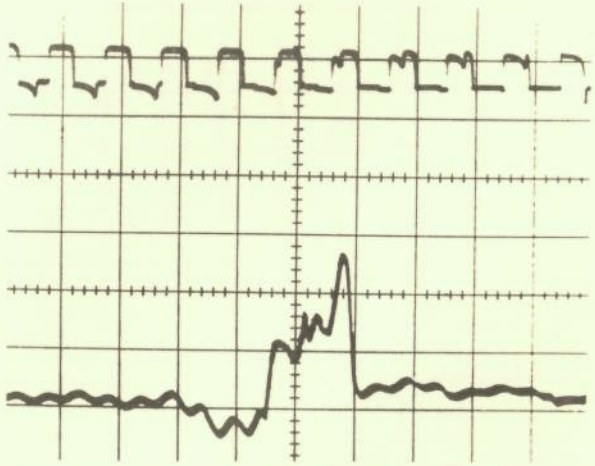

SPEED 1002 R.P.M. LOAD 1500 LBS /INCH FACE WIDTH. SENSITIVITY 2 VOLTS/CMS
HORIZONTAL SWEEP MAGNIFICATION X 10 TIME BASE 10 MILLISEC/CMS

FIG 23

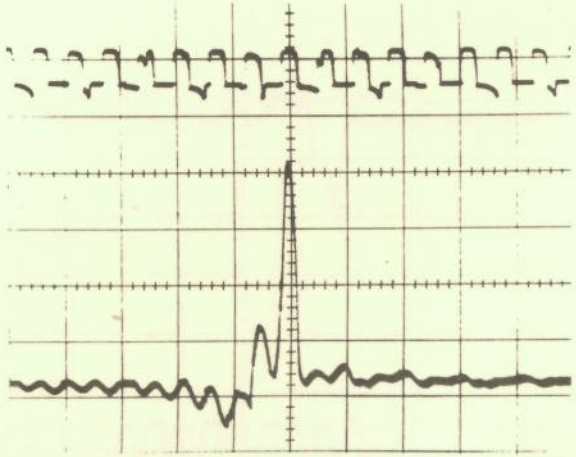

SPEED 1520 R.P.M. LOAD 1500 LBS / INCH FACE WIDTH. SENSITIVITY 2 VOLTS/CMS
HORIZONTAL SWEEP MAGNIFICATION X 10 TIME BASE 10 MILLISEC /CMS

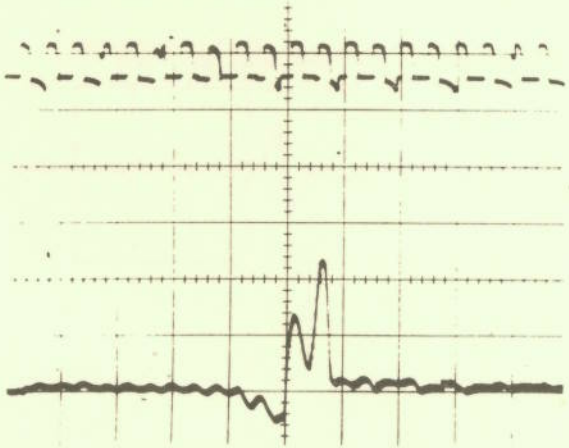

SPEED 2000 R.P.M. LOAD 1500 LBS / INCH FACE WIDTH. SENSITIVITY 2 VOLTS/CMS
HORIZONTAL SWEEP MAGNIFICATION X 10 TIME BASE 10 MILLISEC/CMS

FIG 24

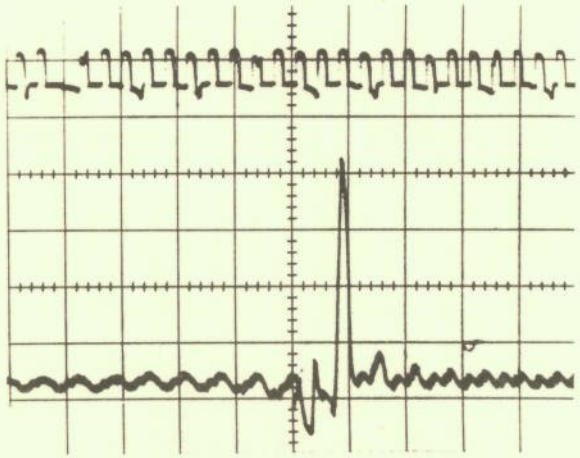

SPEED 2520 R.P.M. LOAD 1500 LBS/INCH FACE WIDTH. SENSITIVITY 2 VOLTS/CMS
HORIZONTAL SWEEP MAGNIFICATION X 10 TIME BASE 10 MILLISEC/CMS

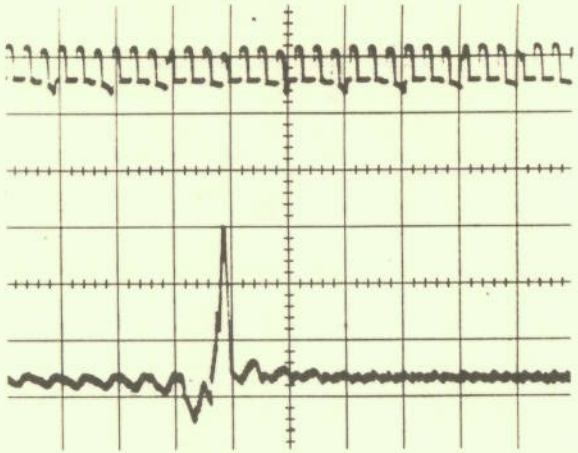

SPEED 3000 R.P.M. LOAD 1500 LBS/INCH FACE WIDTH. SENSITIVITY 2 VOLTS/CMS
HORIZONTAL SWEEP MAGNIFICATION X 10 TIME BASE 10 MILLISEC/CMS

FIG 25

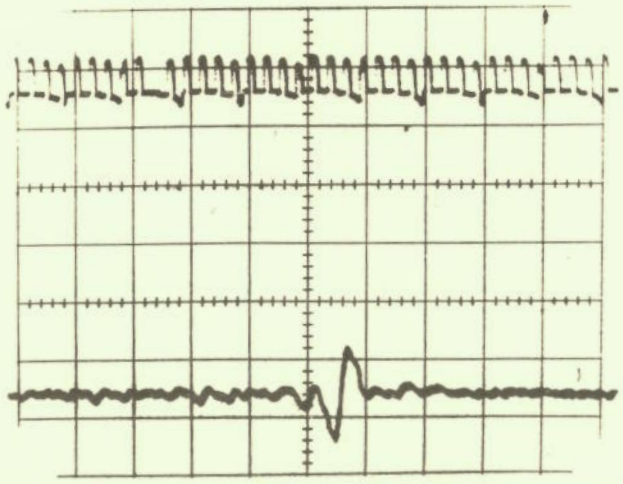

SPEED 3522 R.P.M. LOAD 1500 LBS / INCH FACE WIDTH. SENSITIVITY 2 VOLTS/CMS
HORIZONTAL SWEEP MAGNIFICATION X 10 TIME BASE 10 MILLISEC/CMS

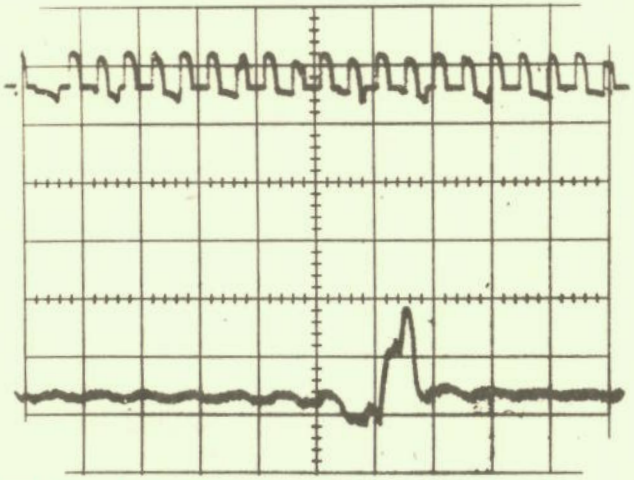

SPEED 4,000 R.P.M. LOAD 15000 LBS/INCH FACE WIDTH. SENSITIVITY 2 VOLTS/CMS
HORIZONTAL SWEEP MAGNIFICATION X 10 TIME BASE 5 MILLISEC/CMS

FIG 26

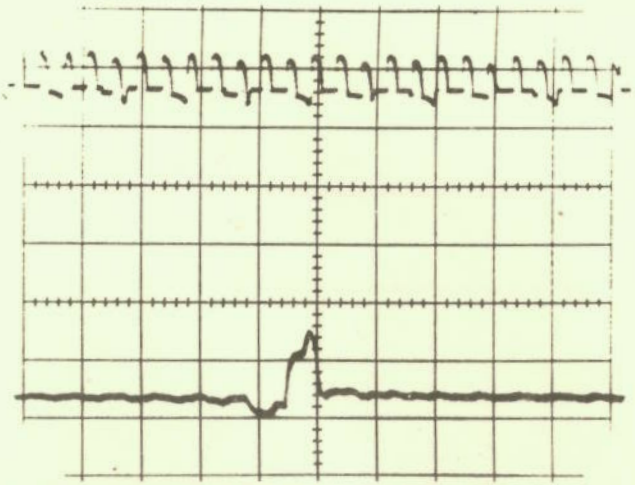

SPEED 4500 R.P.M. LOAD 1500 LBS / INCH FACE WIDTH. SENSITIVITY 2 VOLTS/CMS
HORIZONTAL SWEEP MAGNIFICATION X 10 TIME BASE 5 MILLISEC/CMS

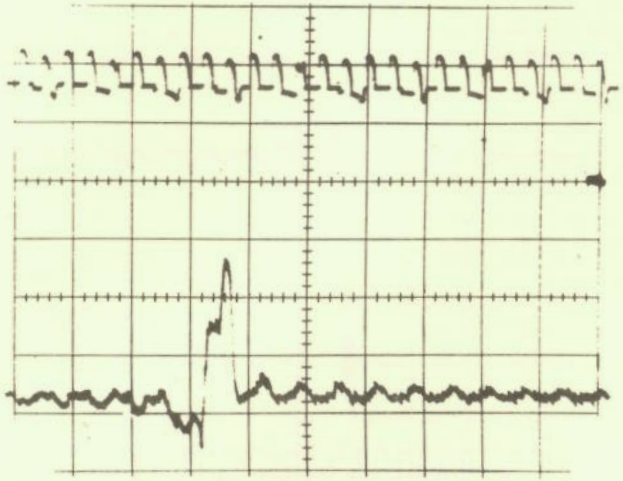

SPEED 4874 R.P.M. LOAD 1500 LBS / INCH FACE WIDTH. SENSITIVITY 1 VOLT/CMS
HORIZONTAL SWEEP MAGNIFICATION X 10 TIME BASE 5 MILLISEC/CMS

FIG 27

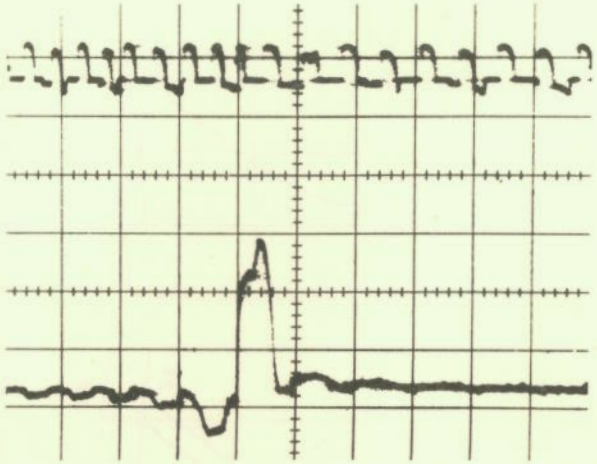

SPEED 4020 R.P.M. LOAD 1500 LBS / INCH FACE WIDTH. SENSITIVITY 0·5 VOLTS/CMS
HORIZONTAL SWEEP MAGNIFICATION X 10 TIME BASE 5 MILLISEC / CMS

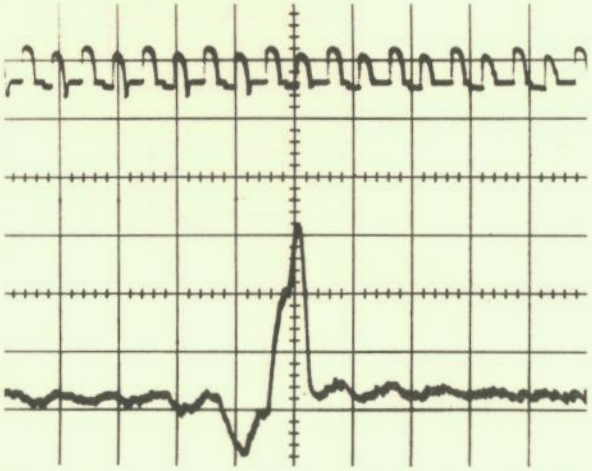

SPEED 3679 R.P.M. LOAD 1500 LBS / INCH FACE WIDTH. SENSITIVITY 0·5 VOLTS / CMS
HORIZONTAL SWEEP MAGNIFICATION X 10 TIME BASE 5 MILLISEC/CMS

FIG 28

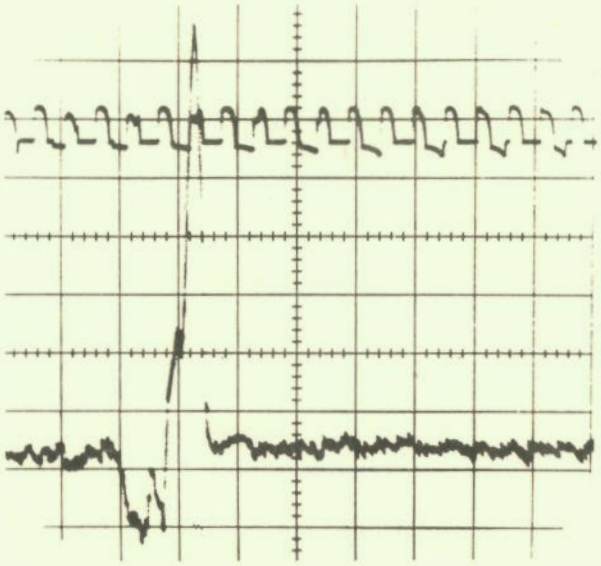

SPEED 3583 R.P.M. LOAD 1500 LBS / INCH FACE WIDTH. SENSITIVITY 0·5 VOLTS / CMS
HORIZONTAL SWEEP MAGNIFICATION X 10 TIME BASE 5 MILLISEC / CMS

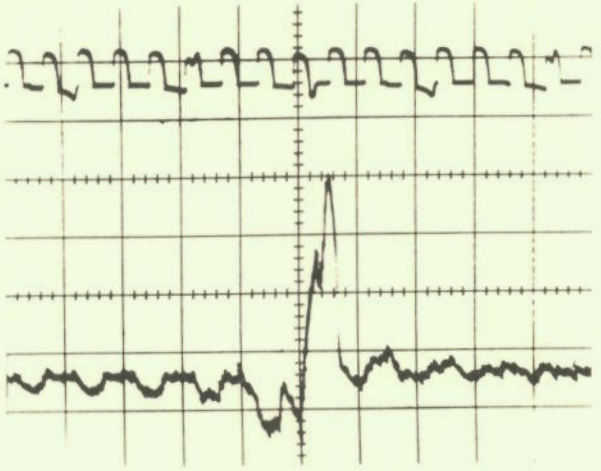

SPEED 3155 R.P.M. LOAD 1500 LBS / INCH FACE WIDTH. SENSITIVITY 0·5 VOLTS / CMS
HORIZONTAL SWEEP MAGNIFICATION X 10 TIME BASE 5 MILLISEC / CMS

FIG 29

TEST GEAR NO 1/1 PRESSURE FACE E. (NO PITCH ERRORS)

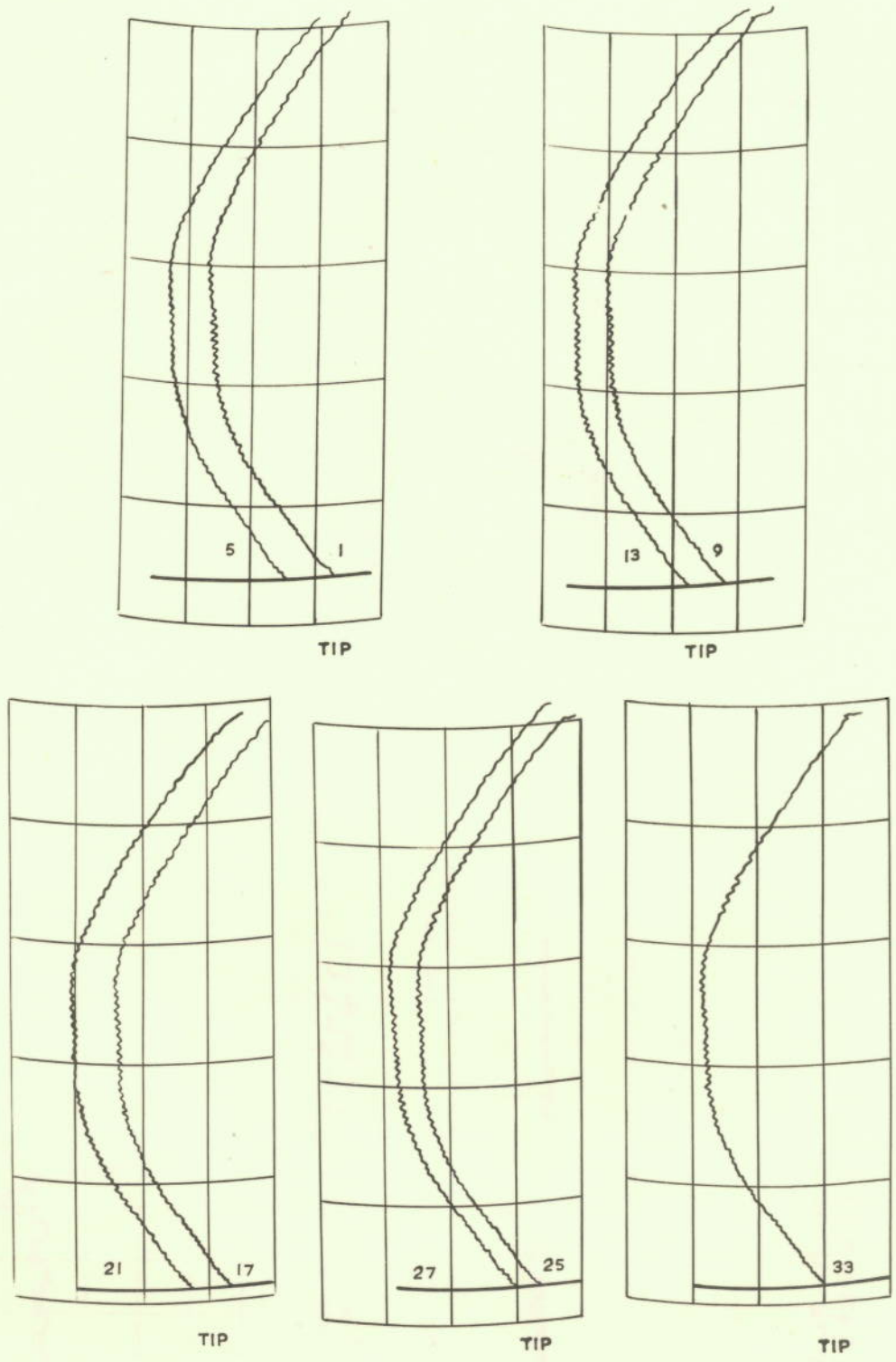

FIG. 30 MAAG PROFILE DIAGRAMS FOR TEST GEARS IS1556/52.

DIAGRAMS TAKEN AT ROLLS ROYCE DERBY IMMEDIATELY AFTER MANUFACTURE

TEST GEAR NO 1/2 PRESSURE FACE E. (NO PITCH ERROR)

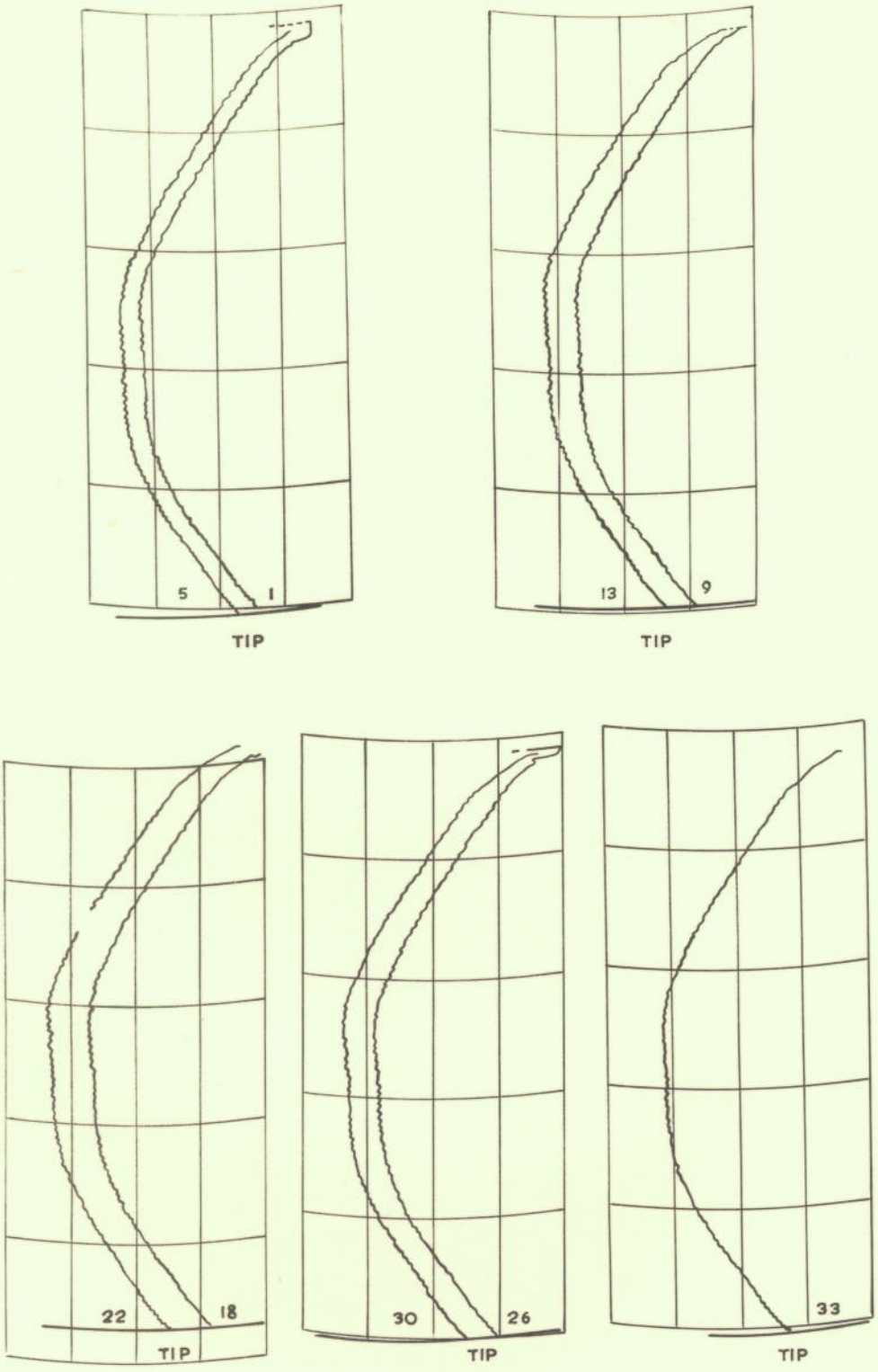

FIG.31. MAAG PROFILE DIAGRAMS FOR TEST GEARS IS1556/52.

DIAGRAMS TAKEN AT ROLLS ROYCE DERBY IMMEDIATELY AFTER MANUFACTURE

TEST GEAR NO 2/1 PRESSURE FACE E. (EQUALLY SPACED.)

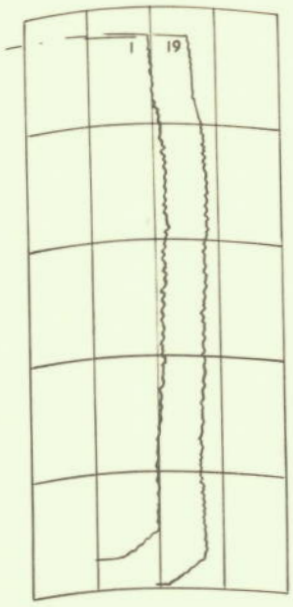

FIG. 32. MAAG PROFILE DIAGRAMS FOR TEST GEARS IS1556/52.

DIAGRAMS TAKEN AT ROLLS ROYCE DERBY IMMEDIATELY AFTER MANUFACTURE.

TEST GEAR NO 2/2 PRESSURE FACE E. (EQUAL SPACING)

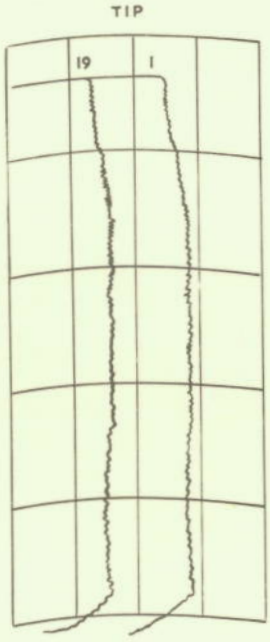

FIG. 33. MAAG PROFILE DIAGRAMS FOR TEST GEARS IS1556/52

DIAGRAMS TAKEN AT ROLLS ROYCE DERBY IMMEDIATELY AFTER MANUFACTURE

TEST GEAR NO 1/1 PRESSURE FACE D. (WITH PITCH ERRORS)

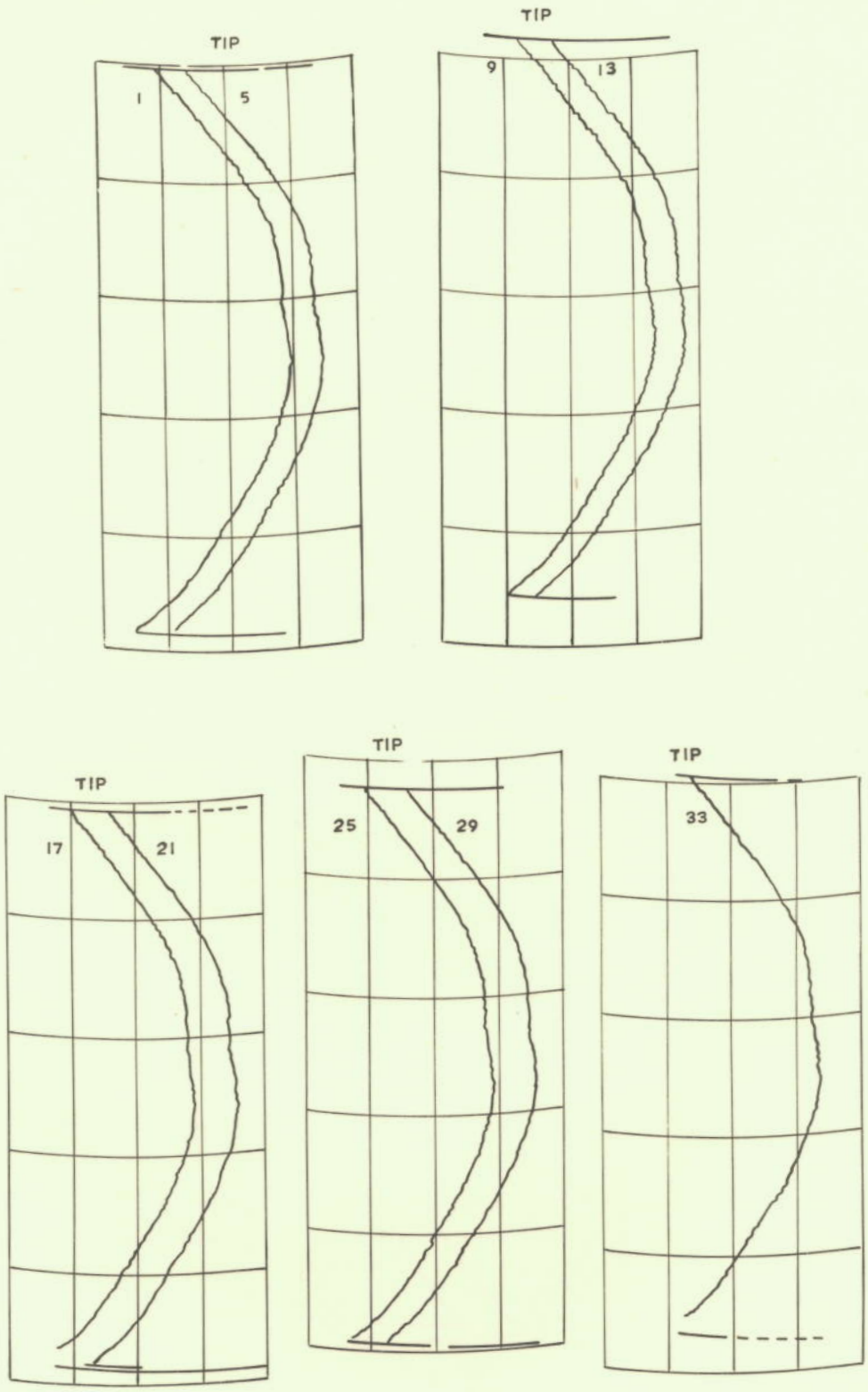

FIG.34. MAAG PROFILE DIAGRAMS FOR TEST GEARS IS1556/52.

DIAGRAMS TAKEN AT ROLLS ROYCE DERBY IMMEDIATELY AFTER MANUFACTURE

TEST GEAR NO 1/2 PRESSURE FACE D. (WITH PITCH ERRORS)

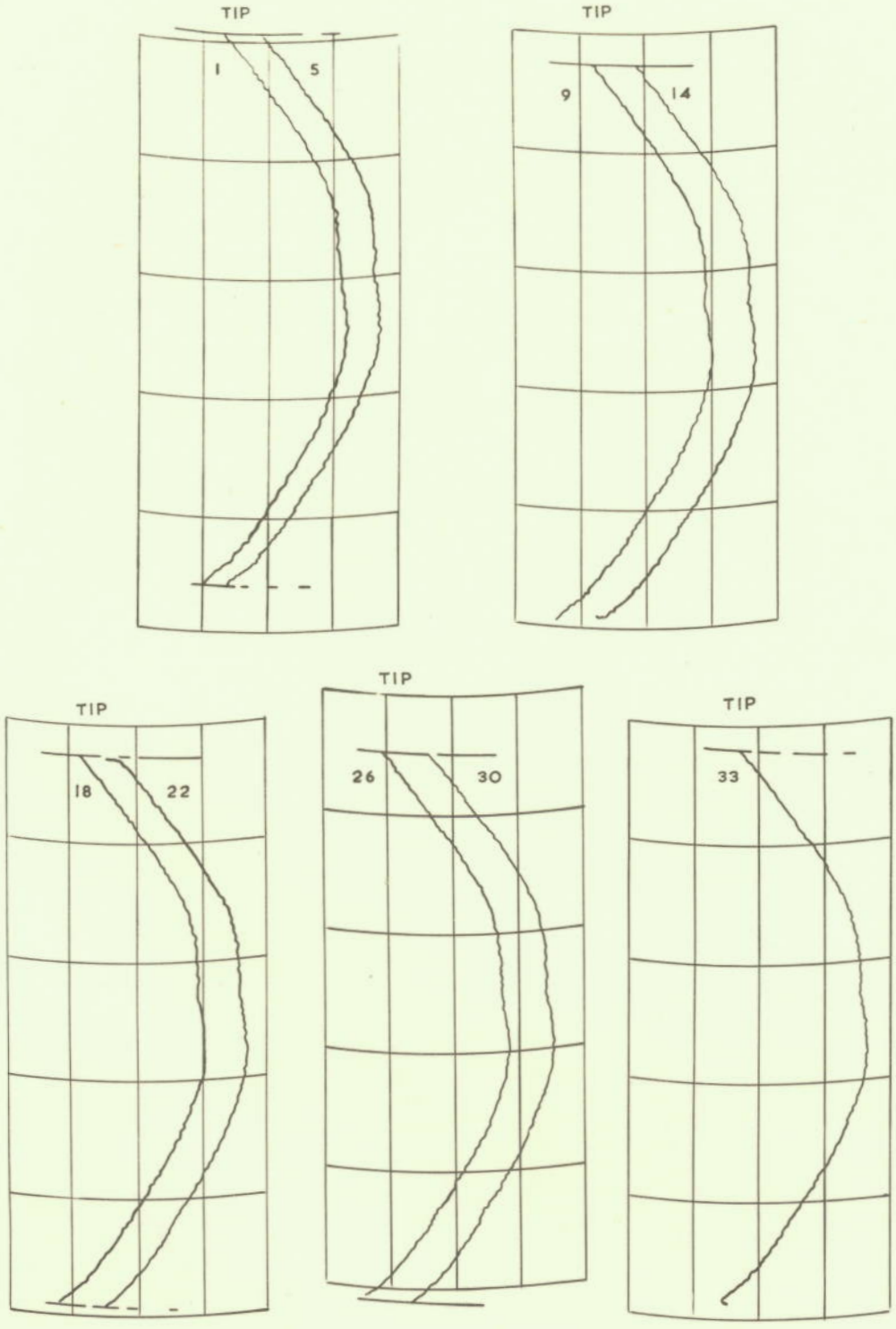

FIG. 35. MAAG PROFILE DIAGRAMS FOR TEST GEARS ISI556/52.

DIAGRAMS TAKEN AT ROLLS ROYCE DERBY IMMEDIATELY AFTER MANUFACTURE

TEST GEAR NO 2/1 PRESSURE FACE D. (WITH PITCH ERRORS)

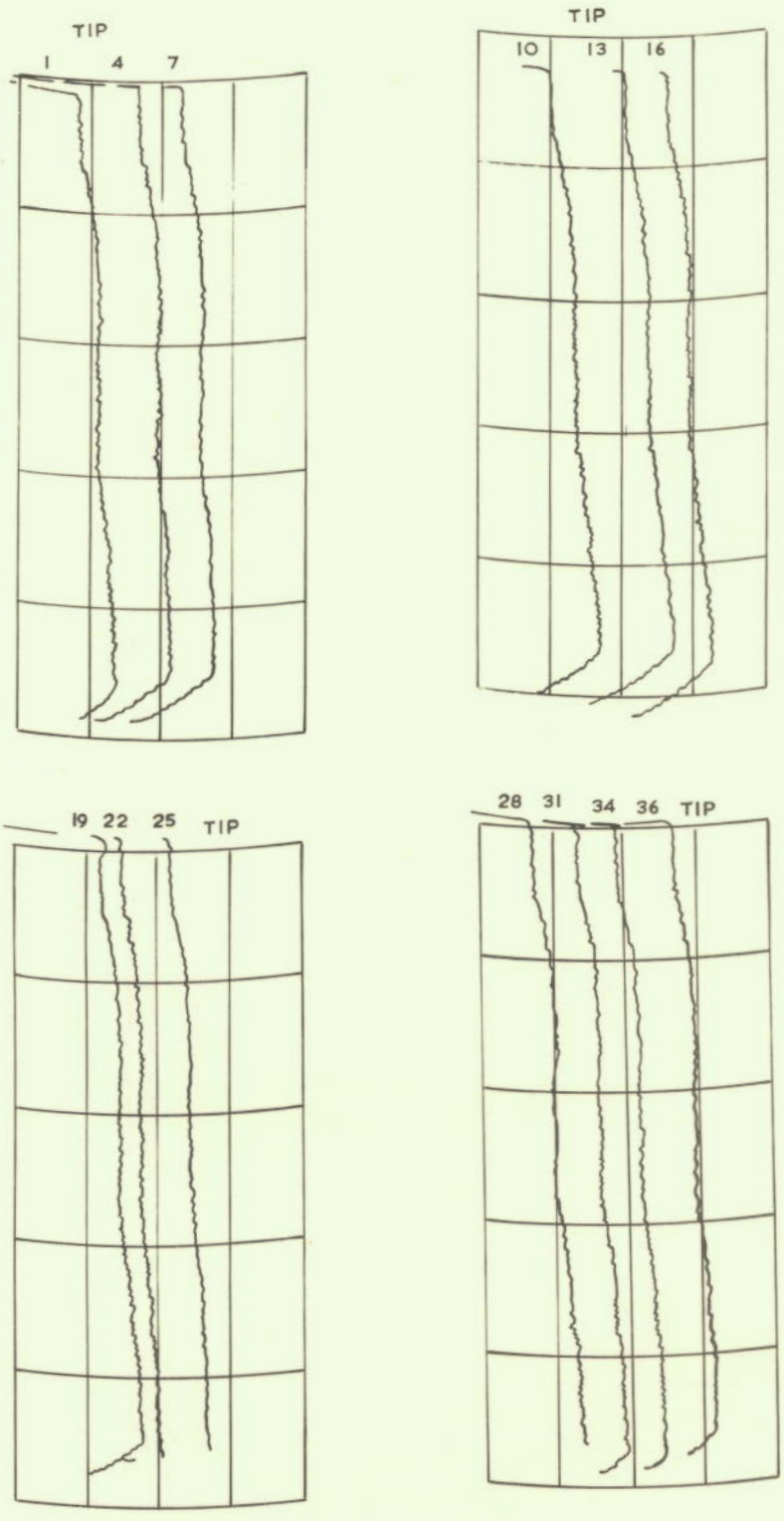

FIG. 36. MAAG PROFILE DIAGRAMS FOR TEST GEARS IS1556/52

DIAGRAMS TAKEN AT ROLLS ROYCE DERBY IMMEDIATELY AFTER MANUFACTURE

TEST GEAR NO 2/2 PRESSURE FACE D. (WITH PITCH ERRORS)

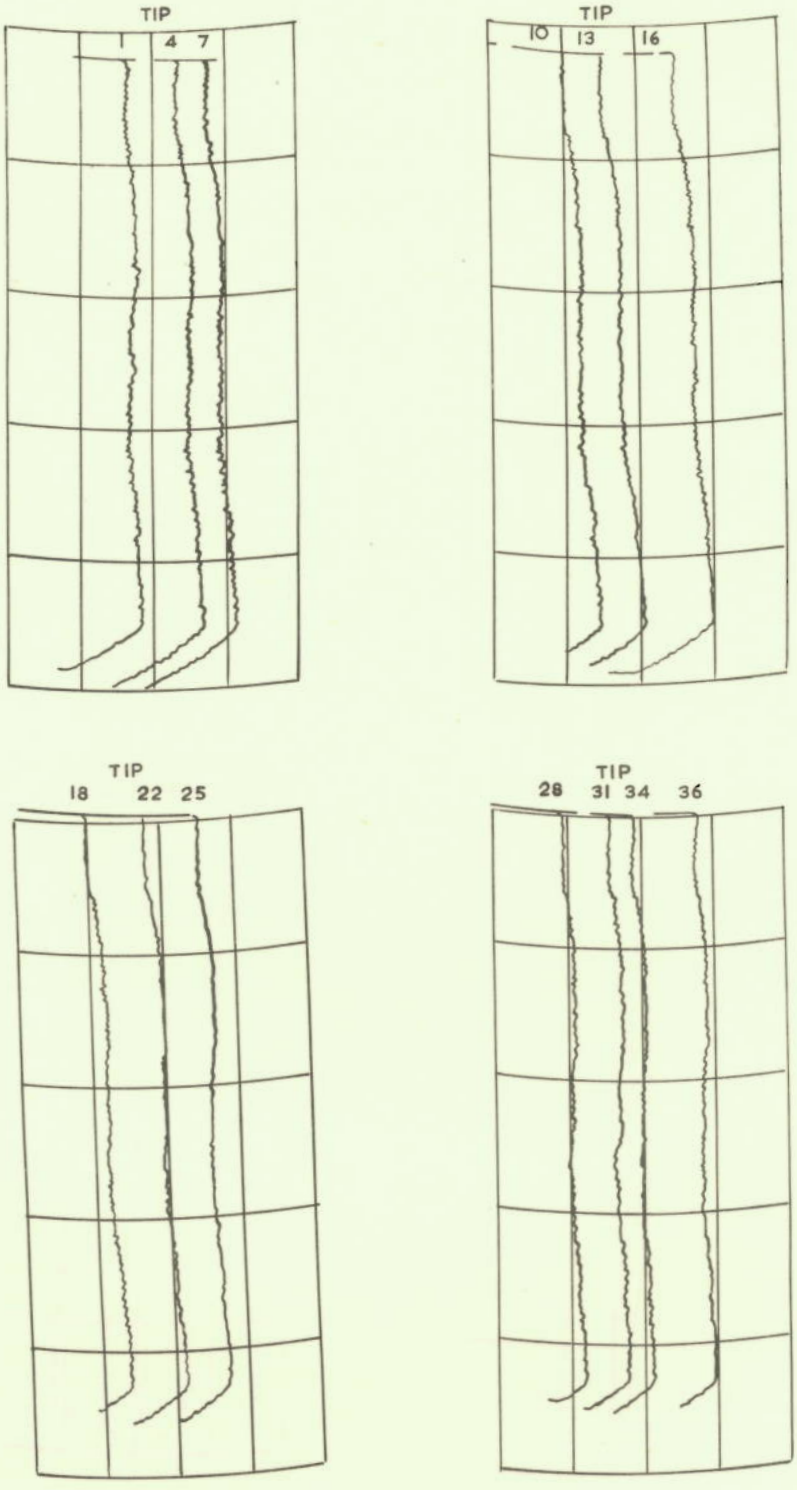

FIG.37. MAAG PROFILE DIAGRAMS FOR TEST GEARS IS1556/52.

DIAGRAMS TAKEN AT ROLLS ROYCE DERBY IMMEDIATELY AFTER MANUFACTURE

GRAPHS

1 - 8 Gear Measurements as determined by Rolls-Royce Ltd.

9 - 12 Gear Measurements as determined by Sigma Instrument Co.

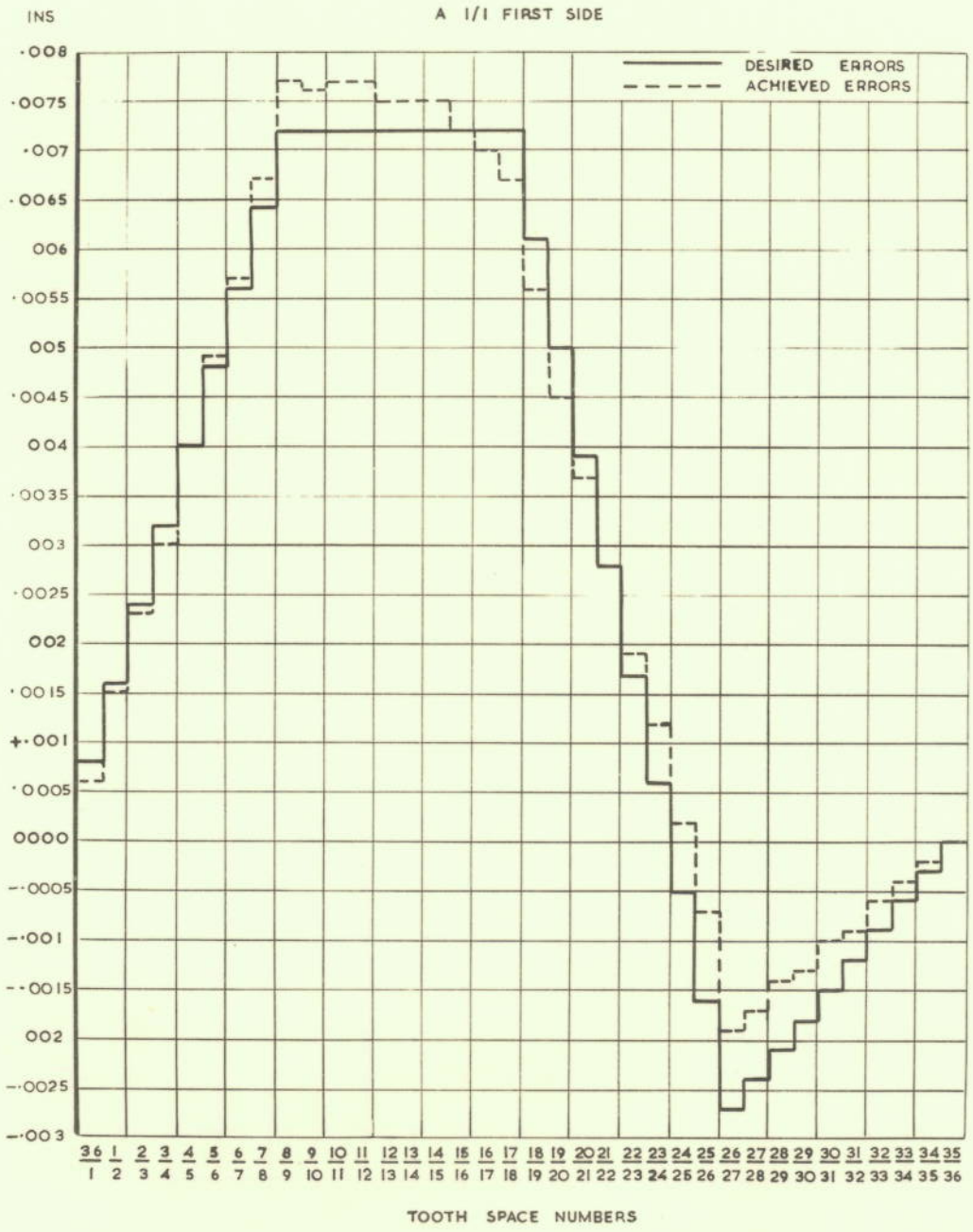

GRAPH. I. GEAR MEASUREMENTS AS DETERMINED BY ROLLS ROYCE

A 1/1 SECOND SIDE

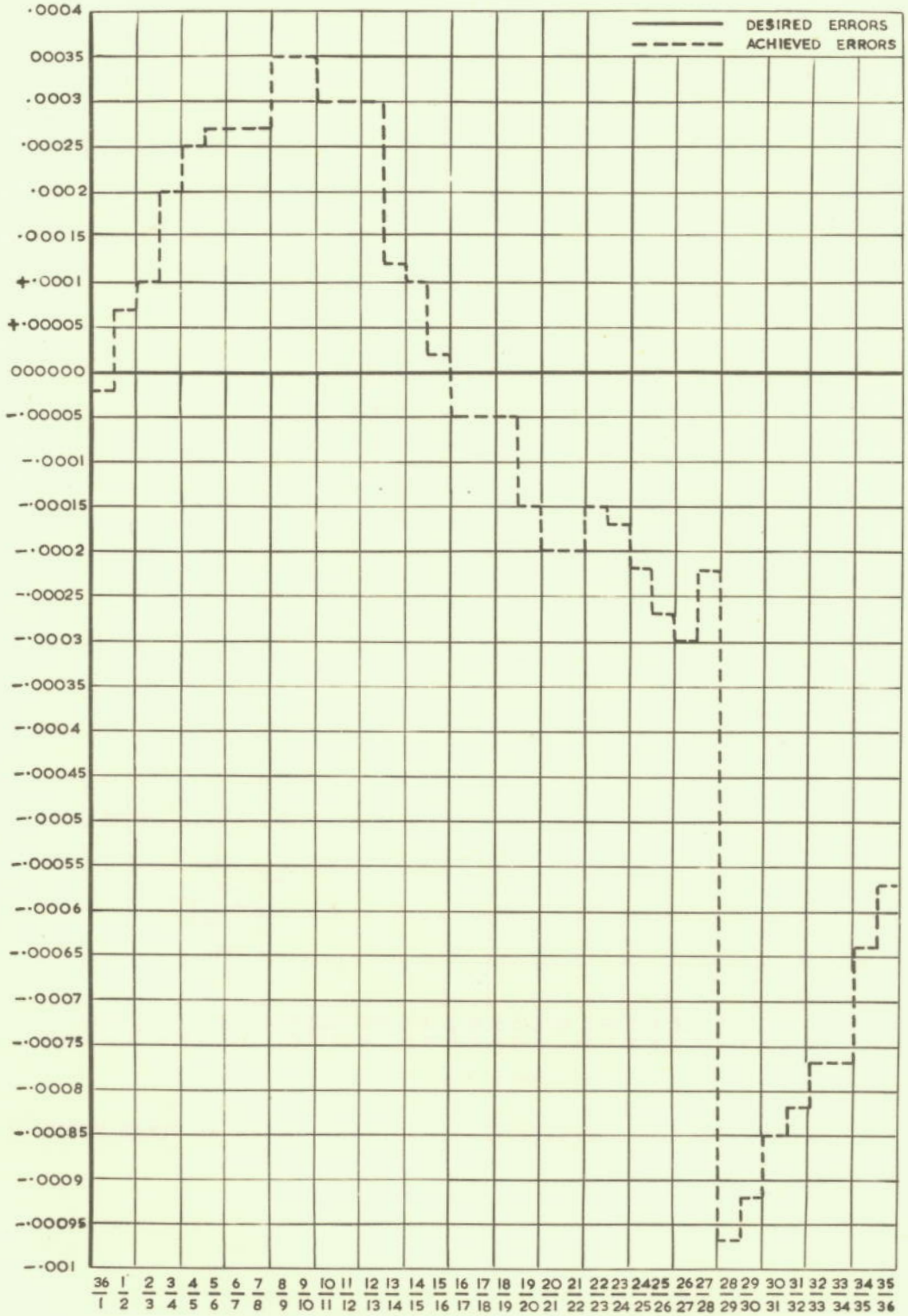

GRAPH. 2. GEAR MEASUREMENTS AS DETERMINED BY ROLLS ROYCE.

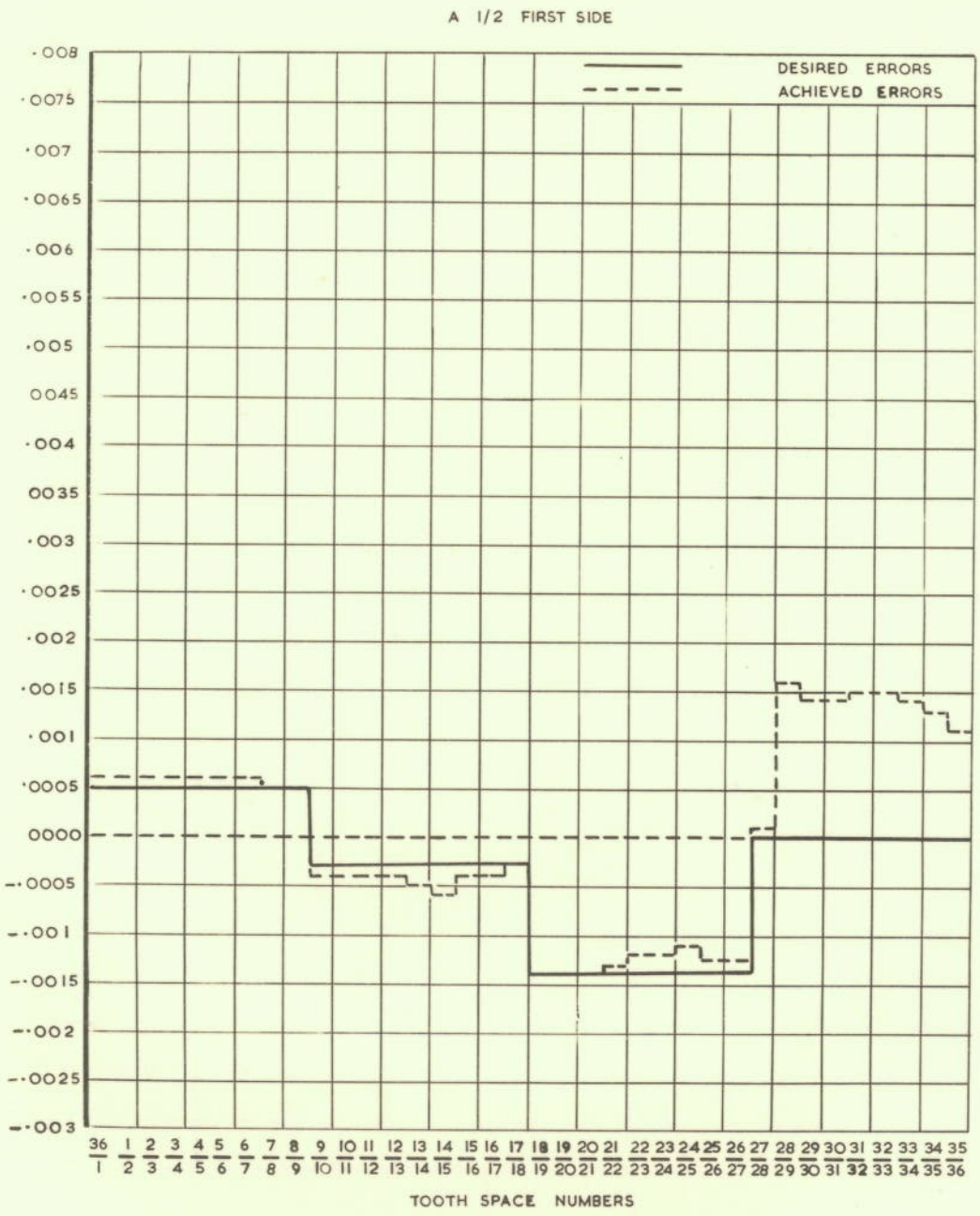

GRAPH. 3. GEAR MEASUREMENTS AS DETERMINED BY ROLLS ROYCE.

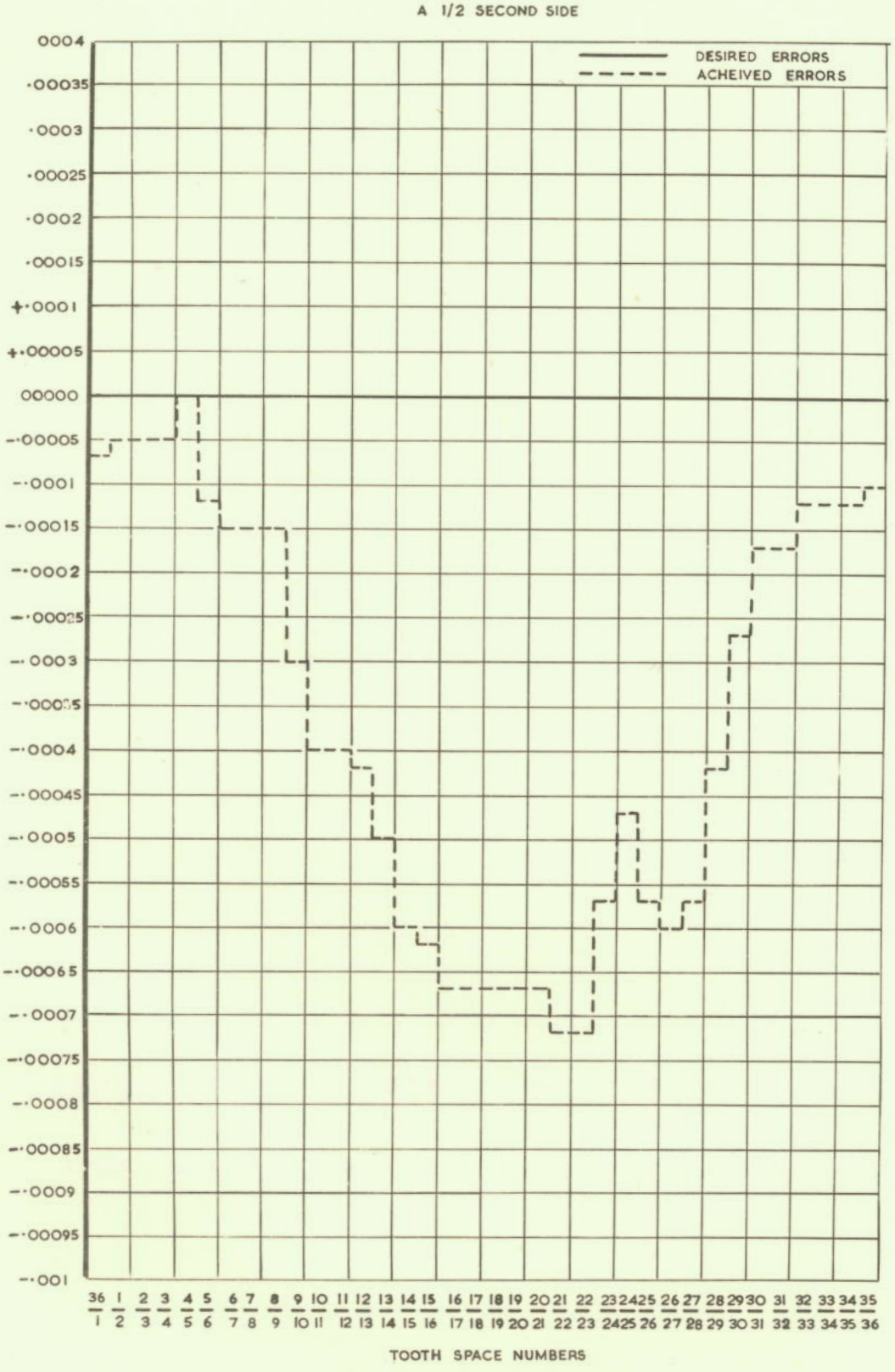

GRAPH. 4. GEAR MEASUREMENTS AS DETERMINED BY ROLLS ROYCE.

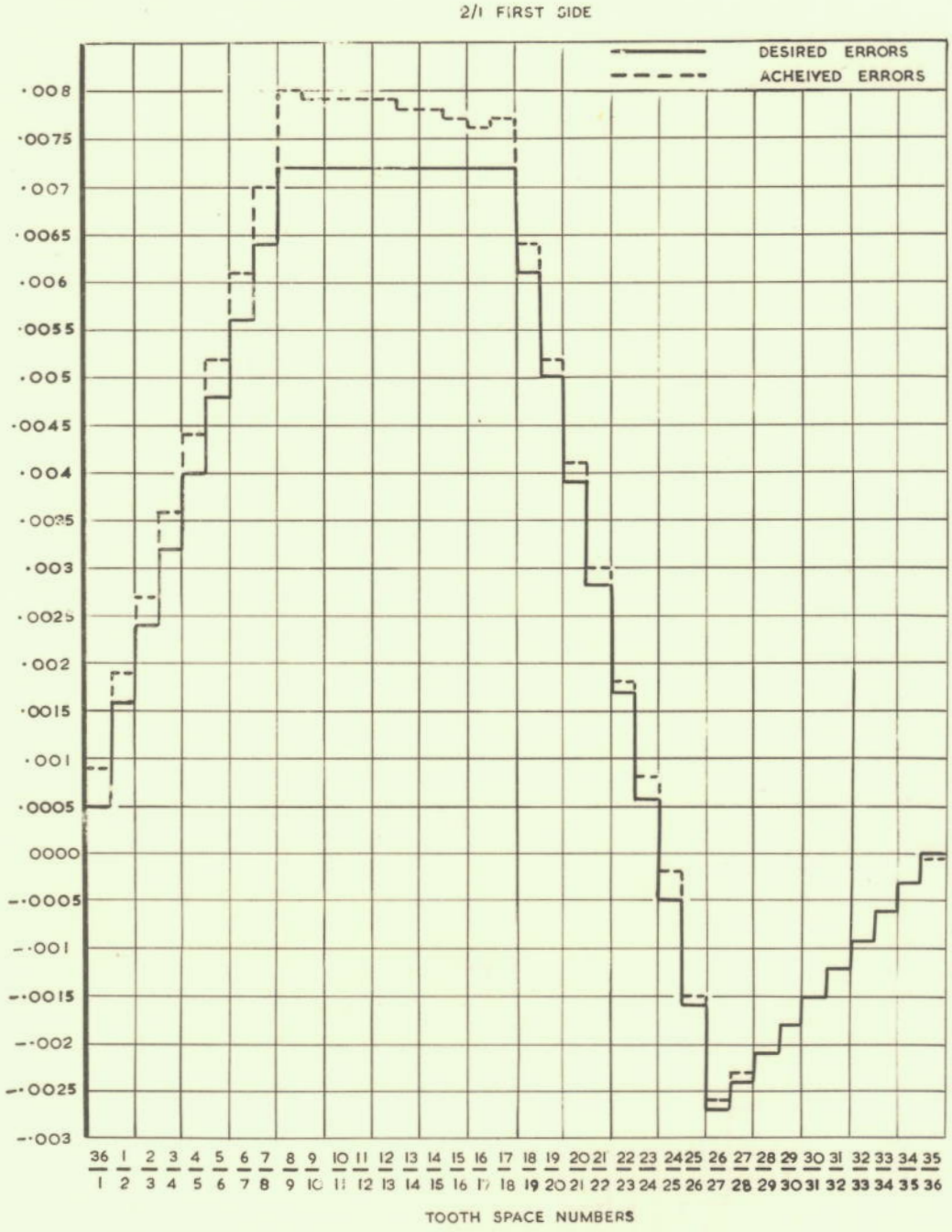

GRAPH. 5. GEAR MEASUREMENTS AS DETERMINED BY ROLLS ROYCE.

2/1 SECOND SIDE

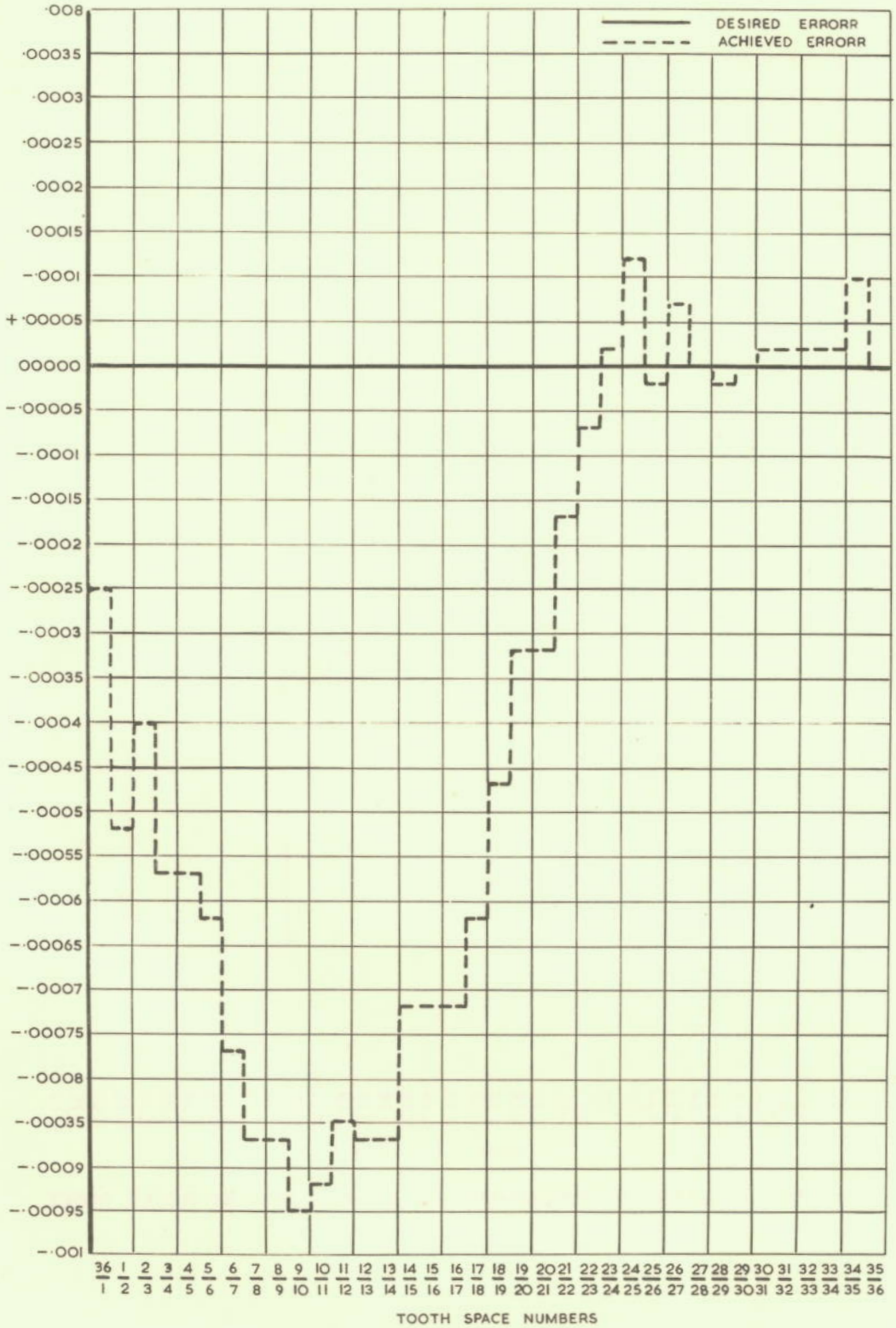

GRAPH. 6. GEAR MEASUREMENTS DETERMINED BY ROLLS ROYCE

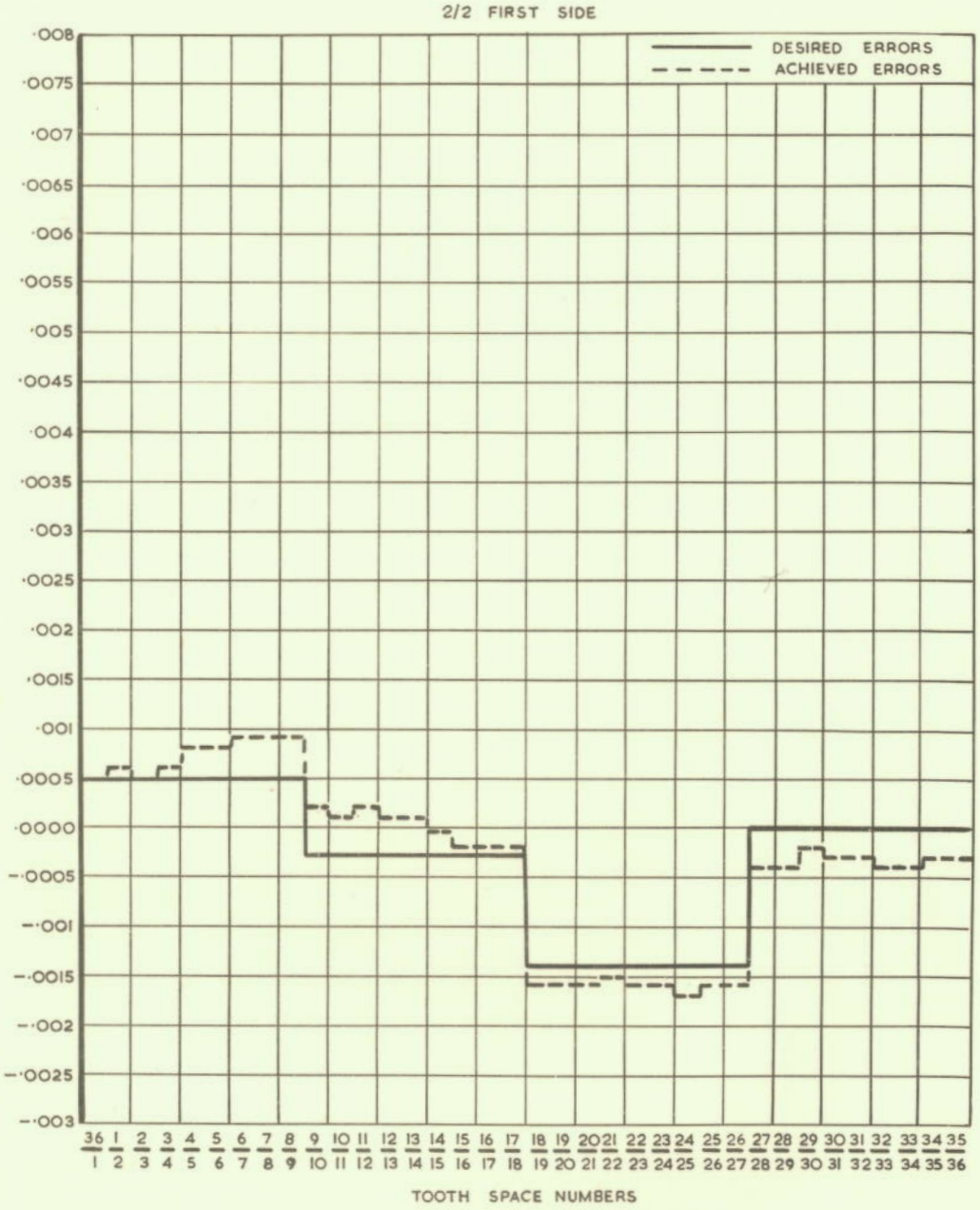

GRAPH. 7. GEAR MEASUREMENTS DETERMINED BY ROLLS ROYCE.

2/2 SECOND SIDE

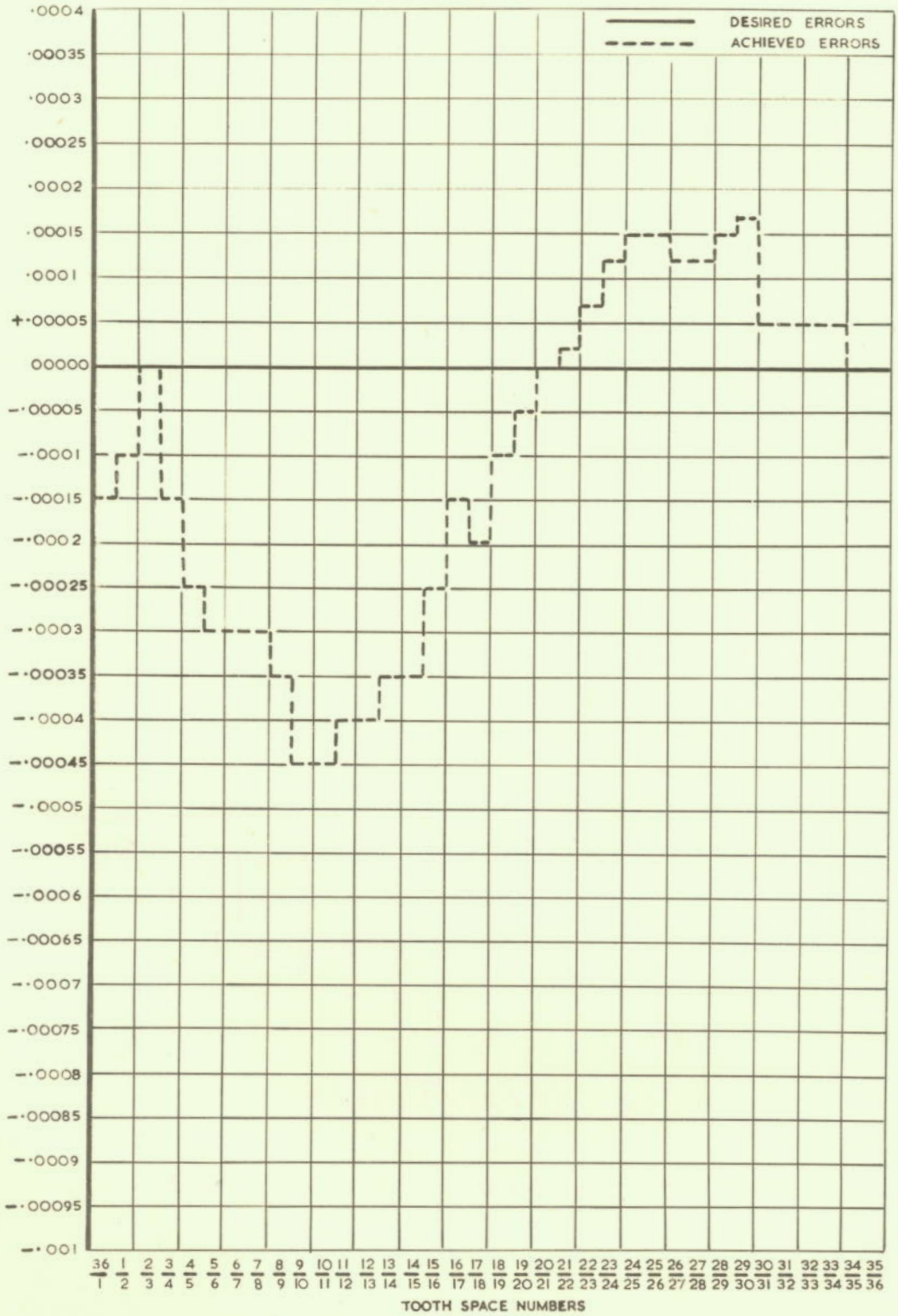

GRAPH 8 GEAR MEASUREMENTS AS DETERMINED BY ROLLS ROYCE

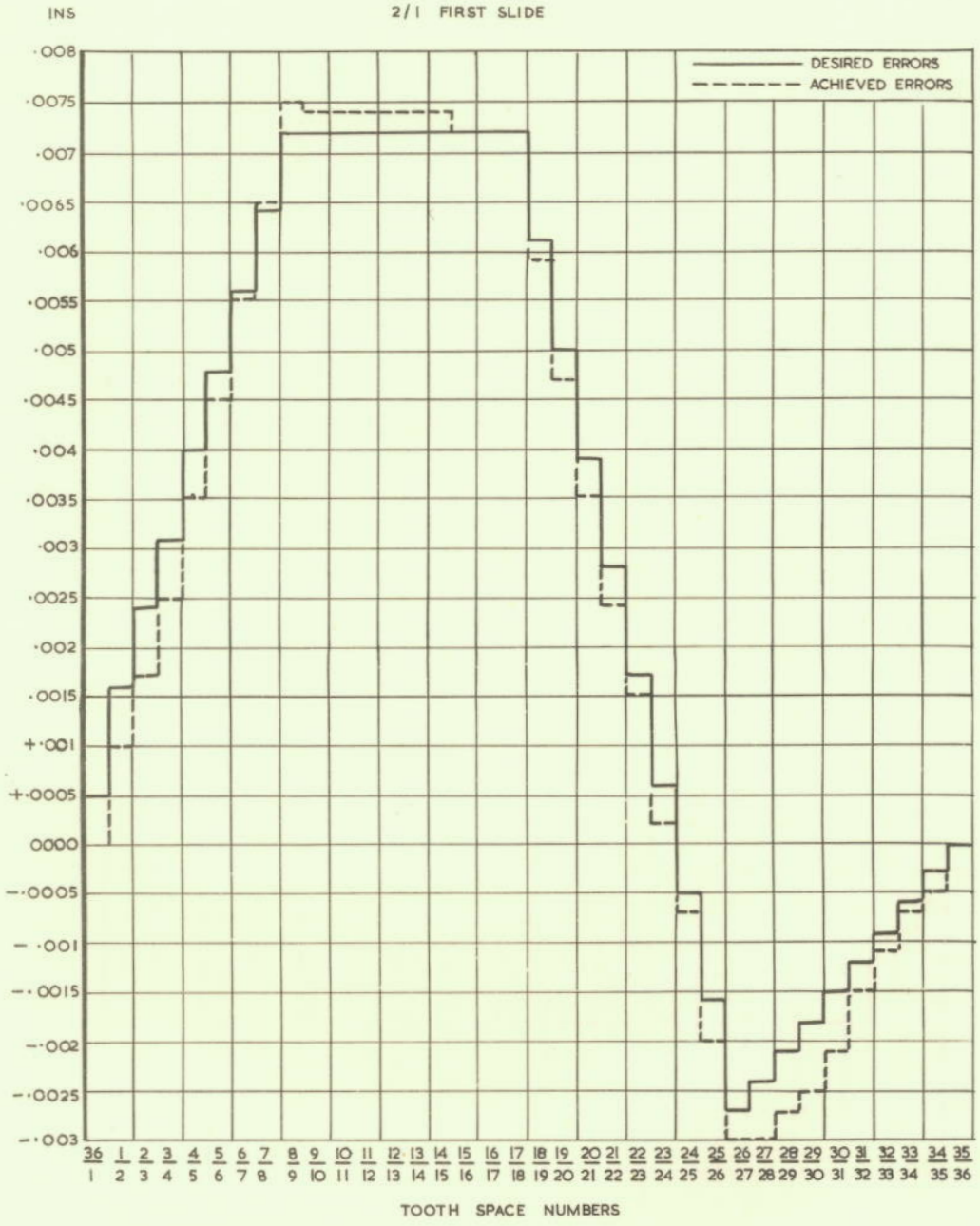

GRAPH. 9. GEAR MEASUREMENTS AS DETERMINED BY SIGMA

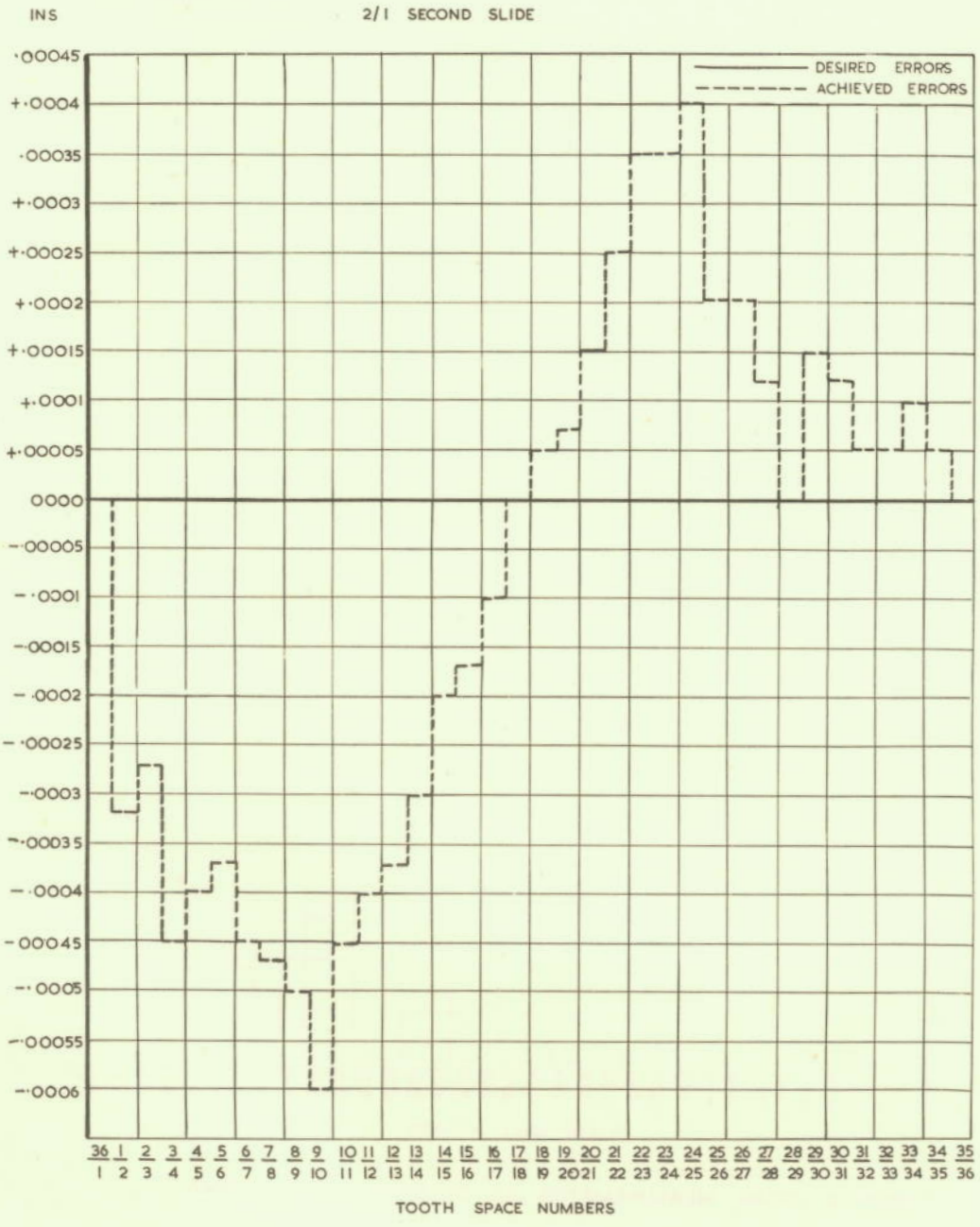

GRAPH. 10. GEAR MEASUREMENTS AS DETERMINED BY SIGMA

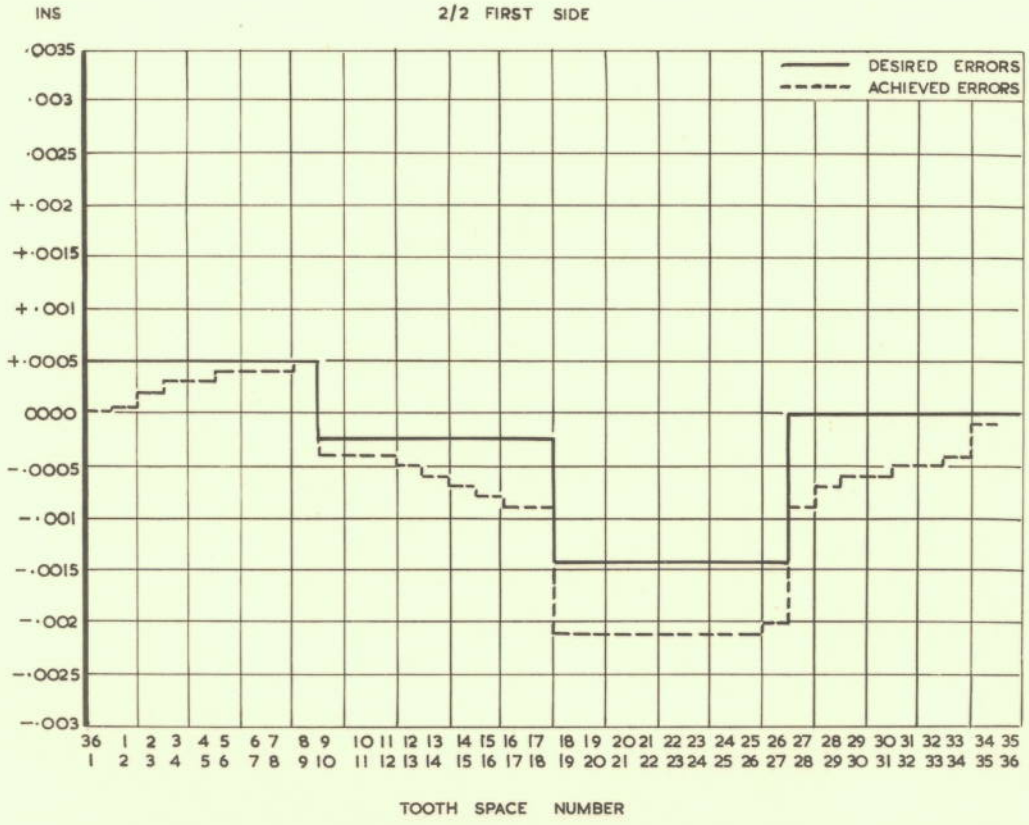

GRAPH. II. GEAR MEASUREMENT AS DETERMINED BY SIGMA

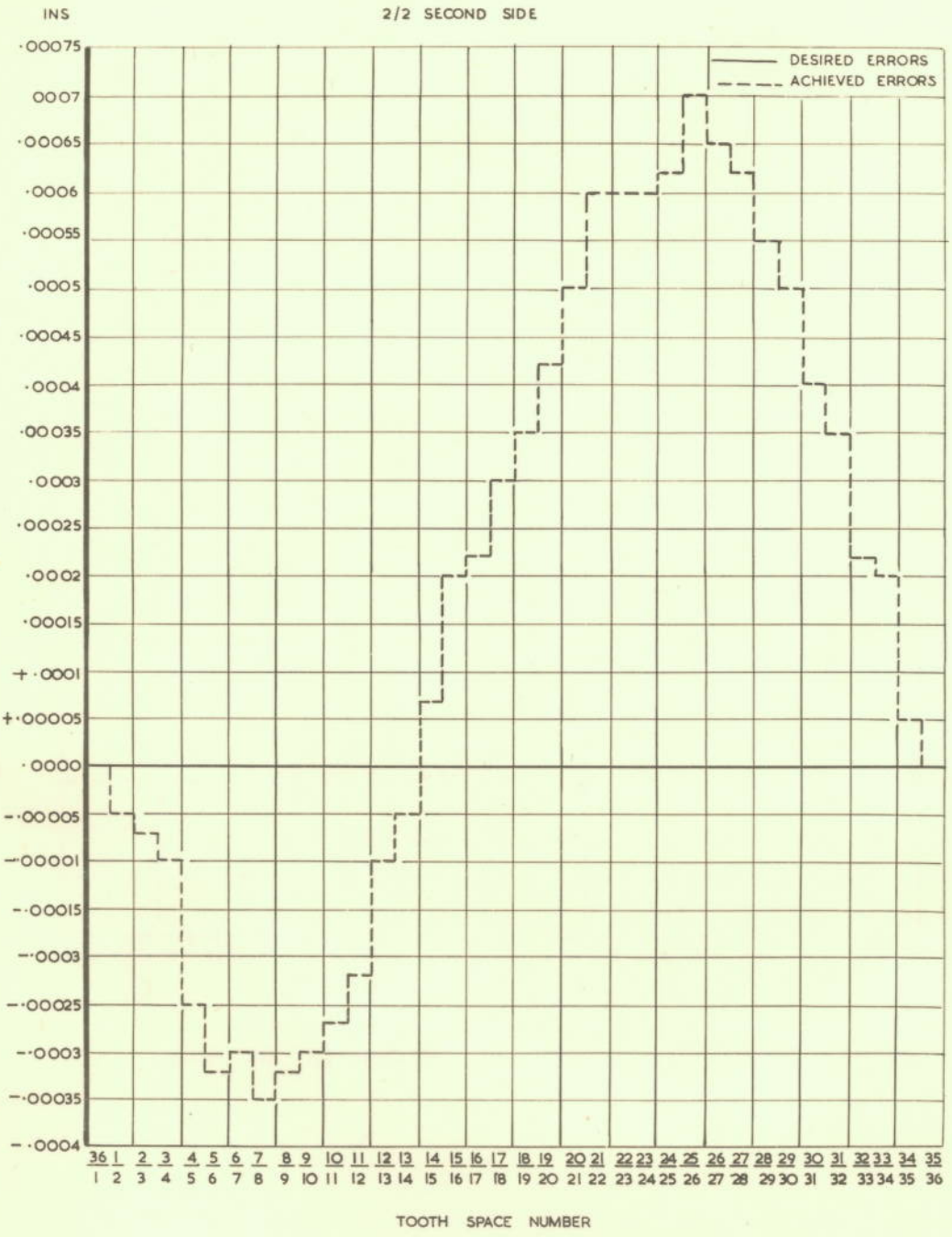

GRAPH. 12, GEAR MEASUREMENTS AS DETERMINED BY SIGMA